

Nanotecnología Aplicada a Biofilms

Nicolás Navarro M.
Químico Farmacéutico

Tabla de Contenidos

1

Definición de Nanotecnología

- Usos en BF bacterianos

Metodologías Síntesis Generales

3

2

Nanotransportadores

Ejemplos Nt

- Lipídicos
- Poliméricos
- Metálicos

4

“Nano-technology’ mainly consists of the processing of separation, consolidation, and deformation of materials by one atom or one molecule.”

—Norio Taniguchi
International Conference on Production
Engineering, 1974, Tokyo.

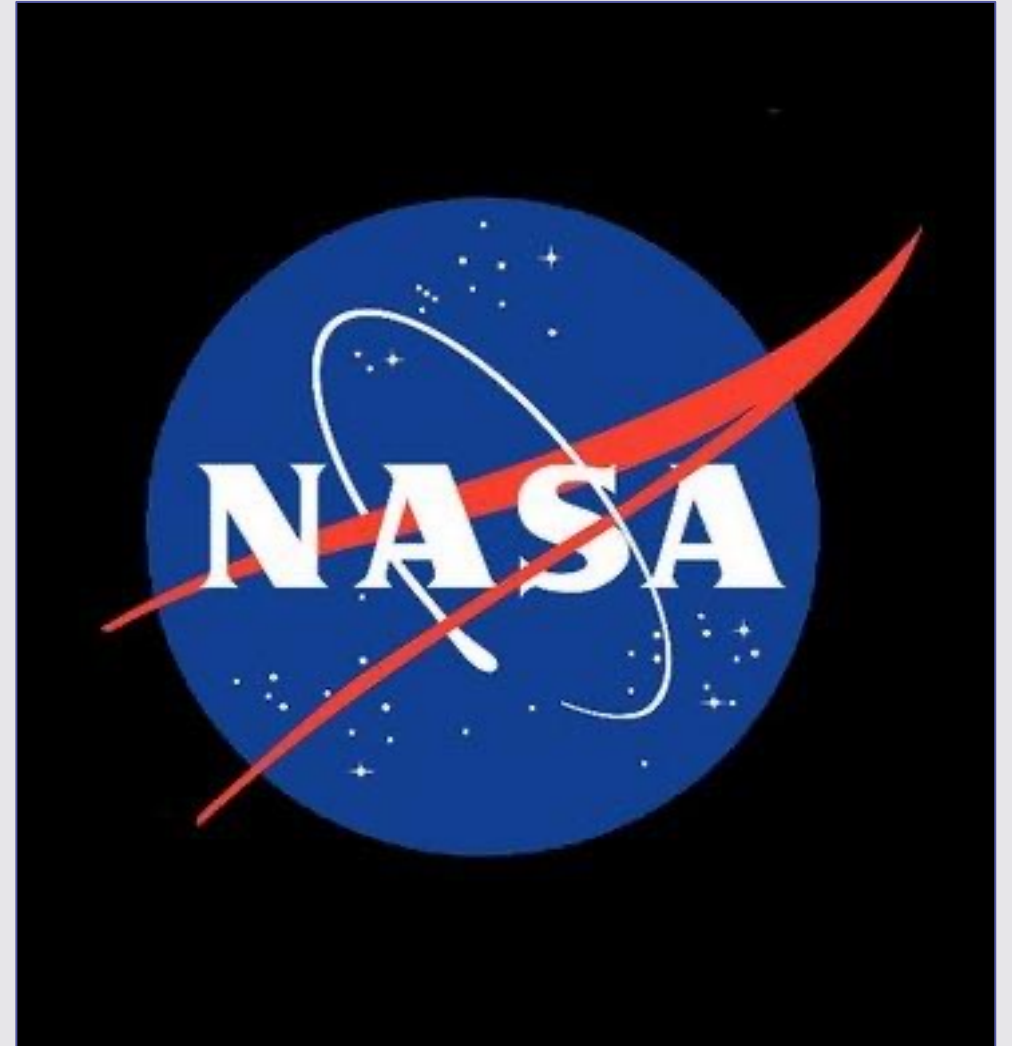


1

Definición de Nanotecnología

INTRODUCCIÓN

“Nanotechnology is the creation of functional materials, devices, and systems through control and manipulation of matter on the nanometer length scale (1-100 nanometers). At this scale, engineers have the ability to exploit novel phenomena and material properties, be they physical, chemical, biological, mechanical, or electrical”

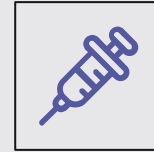


¿De qué manera podemos utilizar la NT para el control de BF?

¿De qué manera podemos utilizar la NT para el control de BF?



**Modificación
Superficial**



**Nanocarriers
ATB/ATM**

¿De qué manera podemos utilizar la NT para el control de BF?

Modificación Superficial



Catéteres centrales de acceso venoso

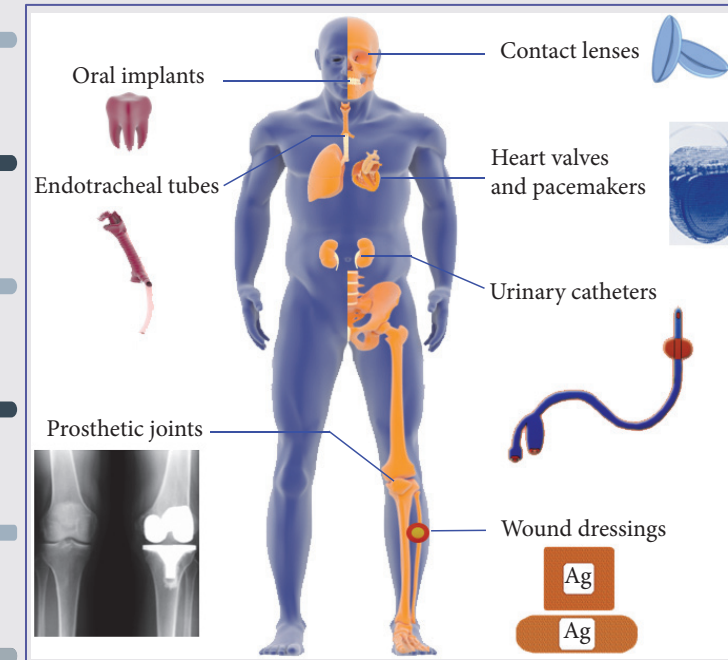
Catéteres urinarios

Tubos endotraqueales

Implantes dentales

Implantes articulares

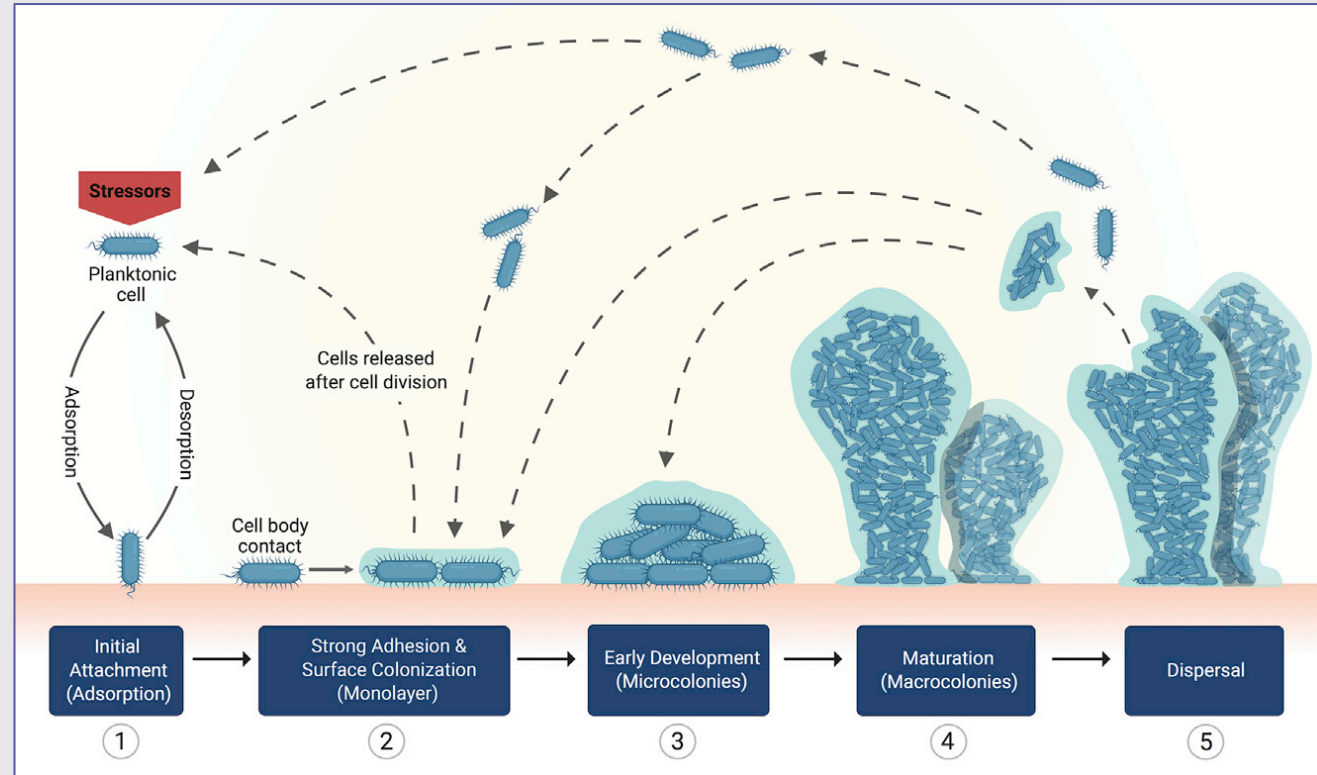
Marcapasos y Válvulas cardiacas



¿De qué manera podemos utilizar la NT para el control de BF?



Modificación Superficial

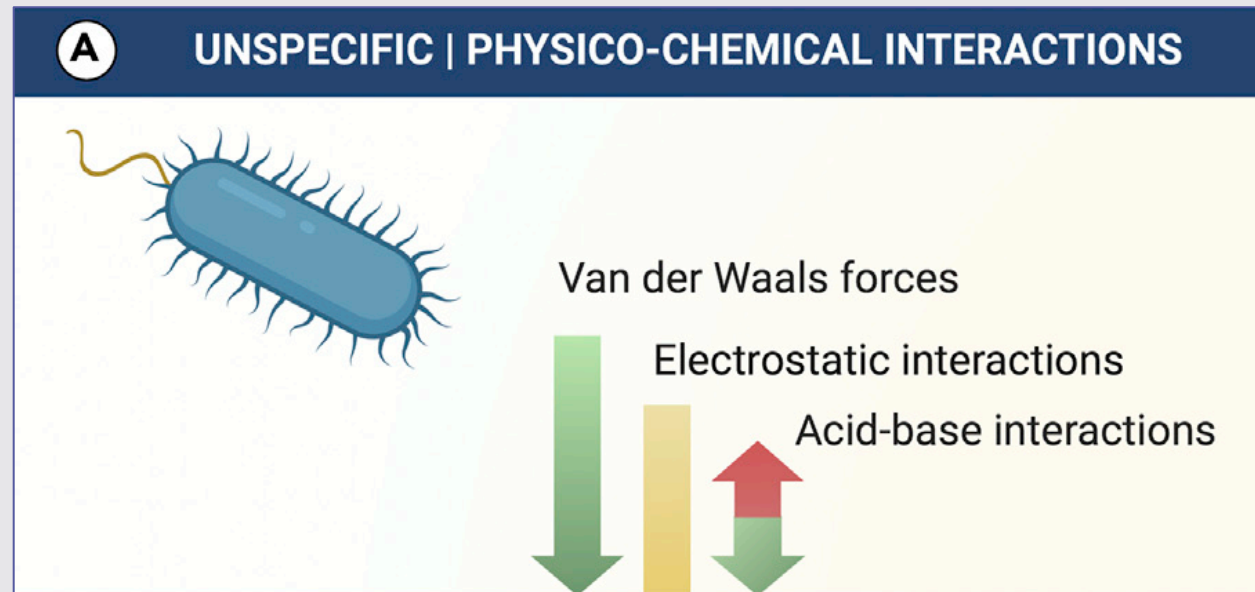


Guzmán-Soto I. et al. Mimicking biofilm formation and development: Recent progress in *in vitro* and *in vivo* biofilm models. iScience. 2021

¿De qué manera podemos utilizar la NT para el control de BF?



Modificación Superficial



Guzmán-Soto I. et al. Mimicking biofilm formation and development: Recent progress in *in vitro* and *in vivo* biofilm models. iScience. 2021

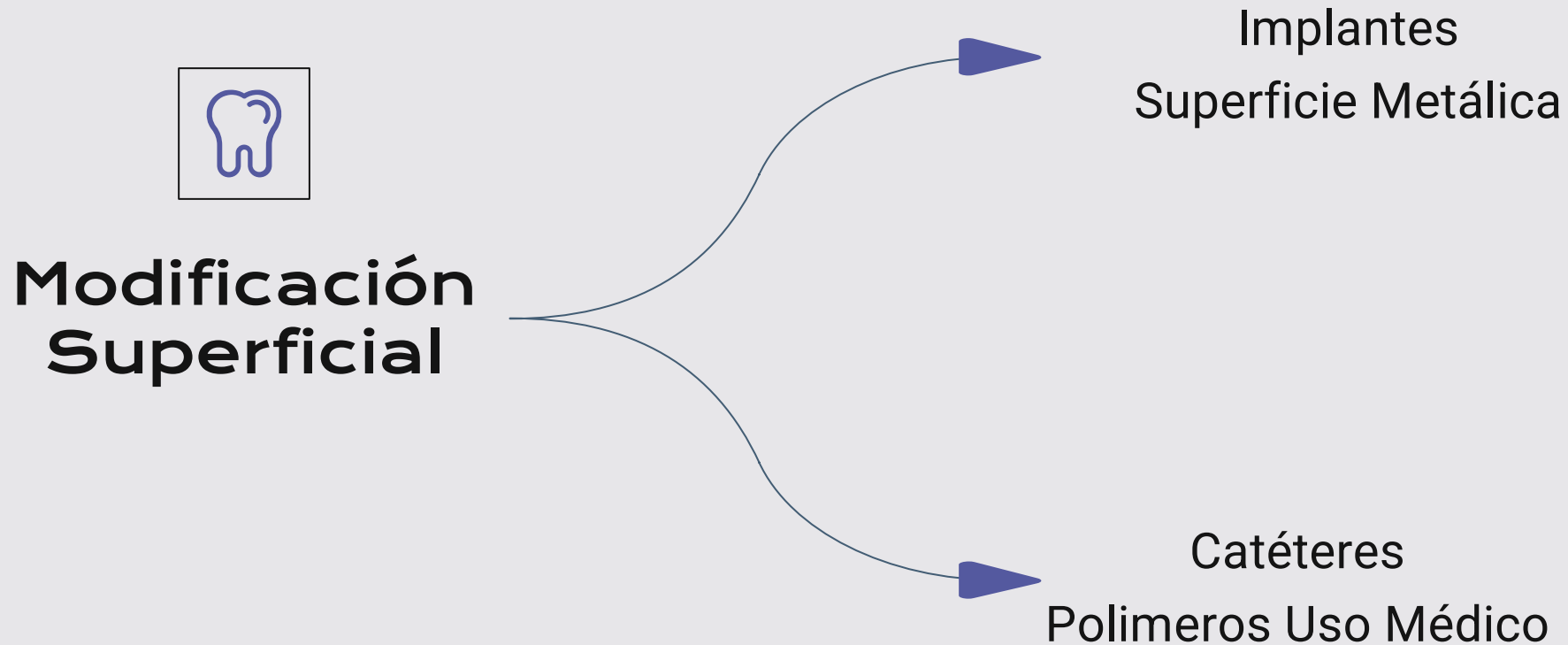
¿De qué manera podemos utilizar la NT para el control de BF?



Modificación Superficial

- 1) *Antifouling coatings* (Dureza, carga, hidrofobicidad)
- 2) Modificaciones antiadhesivas (polímeros)
- 3) Adición de antimicrobianos.
- 4) Modificación físico-química.
- 5) Adición de moléculas bioactivas (QSi).

¿De qué manera podemos utilizar la NT para el control de BF?



Modificación Superficies Metálicas

Table 2 Summary of Implant Coatings			
Implant coating	Example	Studies	Outcome
Carbon coating ¹⁵⁻¹⁸	Currently not on the market; still being investigated	In vitro, in vivo studies, and clinical studies	Improved biologic properties and histocompatibility but studies are still under way
Bisphosphonates ¹⁹⁻²²	Currently not on the market; still being investigated	No long-term studies available	No long-term studies available
Bone stimulating Factors ²³⁻²⁷	Currently not on the market; still being investigated	Pilot animal studies and clinical studies	Studies are still under way
Bioactive glasses and ceramics ²⁸⁻³⁰	Currently not on the market; still being investigated	Chemical, in vivo, and in vitro studies	Studies are still under way
Fluoride coatings ³¹	OsseoSpeed	In vitro studies	Selective osteoblast differentiation results
Hydroxyapatite (HA) ³²⁻³⁶	Restore Implant system	In vivo, in vitro, and retrieval studies	Most commonly used type of implant coating; other implant coating studies mainly use HA as a control
Titanium/titanium nitride ³⁷⁻⁴¹	IonFusion	In vitro, in vivo, and clinical studies	Titanium mechanical properties are considered in relation to the degree of osseointegration

Xuereb M, et al. Int J Prosthodont. 2015 Jan-Feb;28(1):51-9.

Modificación Superficies Metálicas

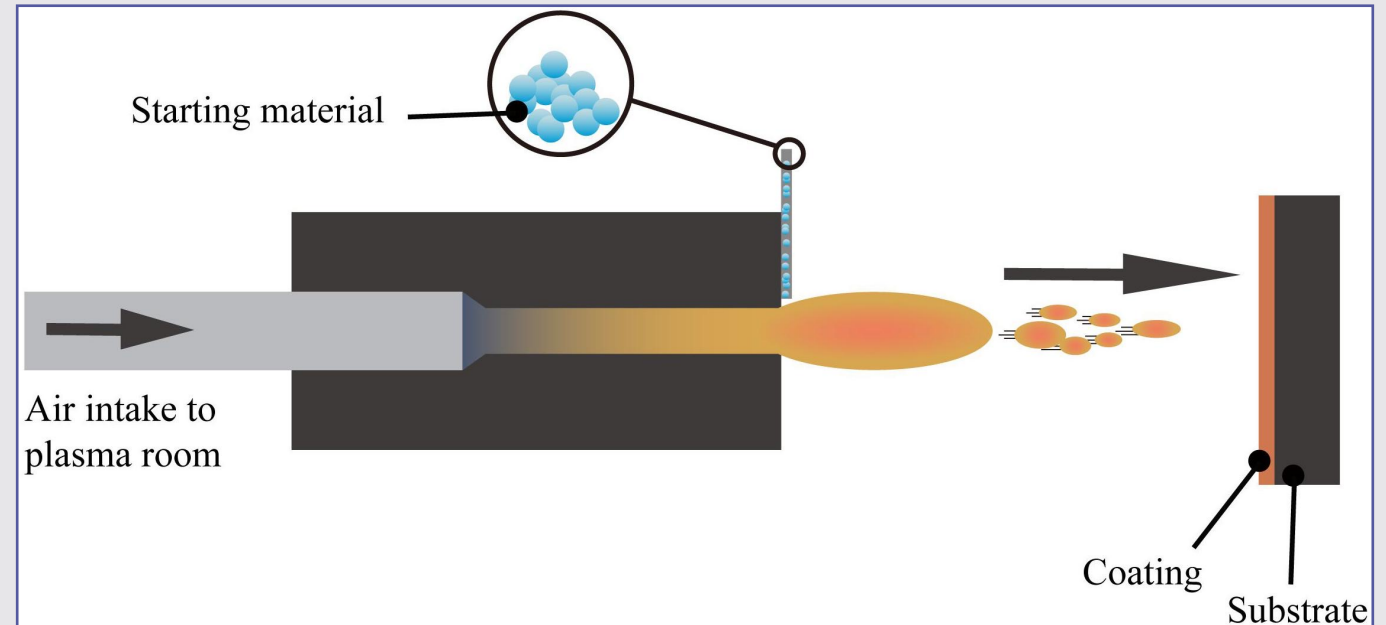
Plasma Spraying

Electrochemical
Anodization

Xuereb M, et al. Int J Prosthodont. 2015 Jan-Feb;28(1):51-9.

Plasma Spraying

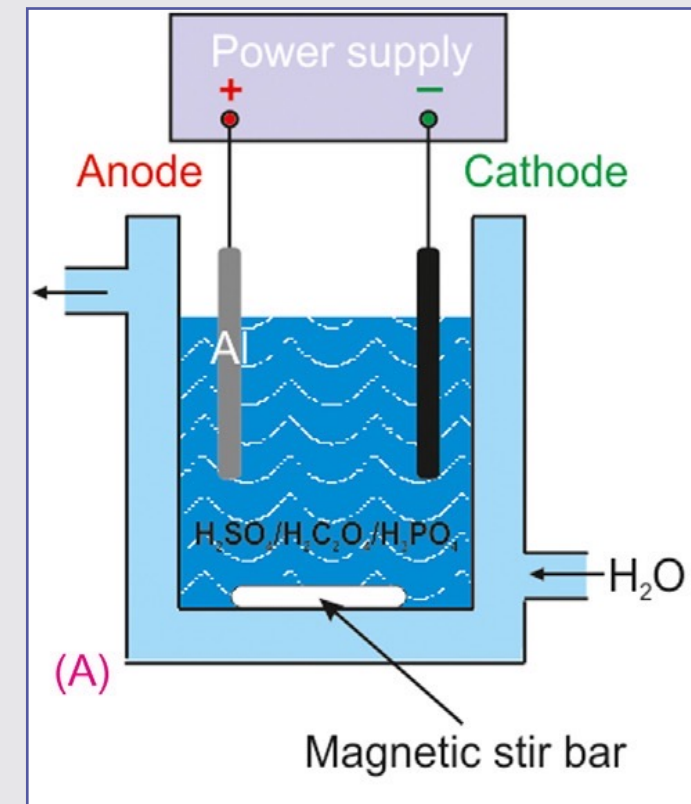
- Gold Estándar.
- Cerámicas (HA) y Metales.
- Recubrimiento Nanométrico.
- Gran estabilidad y control.
- Alta eficiencia de deposición y baja porosidad.



Liu Jianqiao, et al. Frontiers in Bioengineering and Biotechnology, (8), 1314, 2020.

Electrochemical Anodization

- Películas de óxido anódicas.
- Morfología compacta, nanoporosa o nanotubular.
- Dopaje metales (Zn, Ag, Au, Cu, etc).
- Modificación estructural.
- Bajo costo.
- Escalabilidad técnica.



Grzegorz D. Sulka, Chapter one - Introduction to anodization of metals, In Micro and Nano Technologies, Nanostructured Anodic Metal Oxides, Elsevier, 2020, Pages 1-34.

Electrochemical Anodization

Formación de nanotubos en superficie de implantes de titanio.

- Bajo costo
- Control de características superficiales
 - El diámetro del nanotubo se puede controlar mediante el voltaje de oxidación.
 - La longitud del nanotubo se controla mediante la combinación del tiempo de oxidación, la temperatura de oxidación y el valor de pH del electrolito.

Liu Jianqiao, et al. Frontiers in Bioengineering and Biotechnology, (8), 1314, 2020.

Electrochemical Anodization

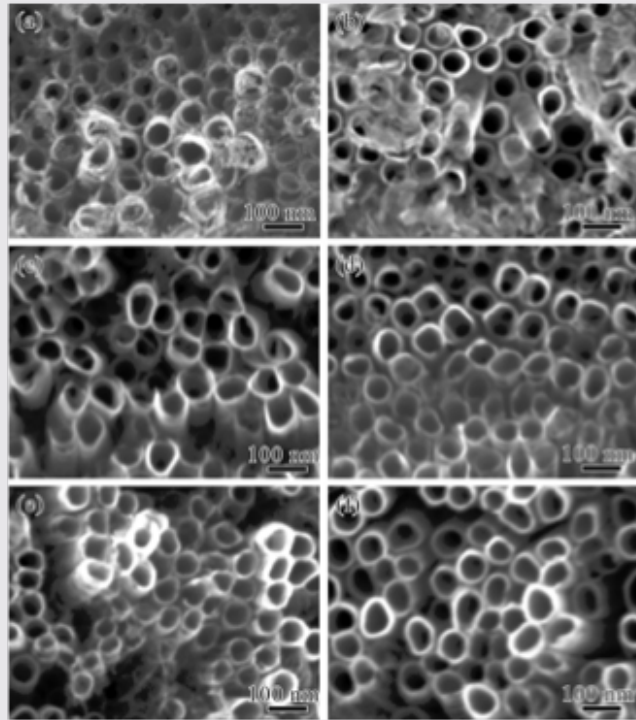


Figure 4. FE-SEM images representing the top view of ZnO-TNTs. (a) Undoped TNTs (spray-gold), (b) 1 mM · L⁻¹ ZnO-TNTs, (c) 2 mM · L⁻¹ ZnO-TNTs, (d) 3 mM · L⁻¹ ZnO-TNTs, (e) 4 mM · L⁻¹ ZnO-TNTs, (f) 5 mM · L⁻¹ ZnO-TNTs.

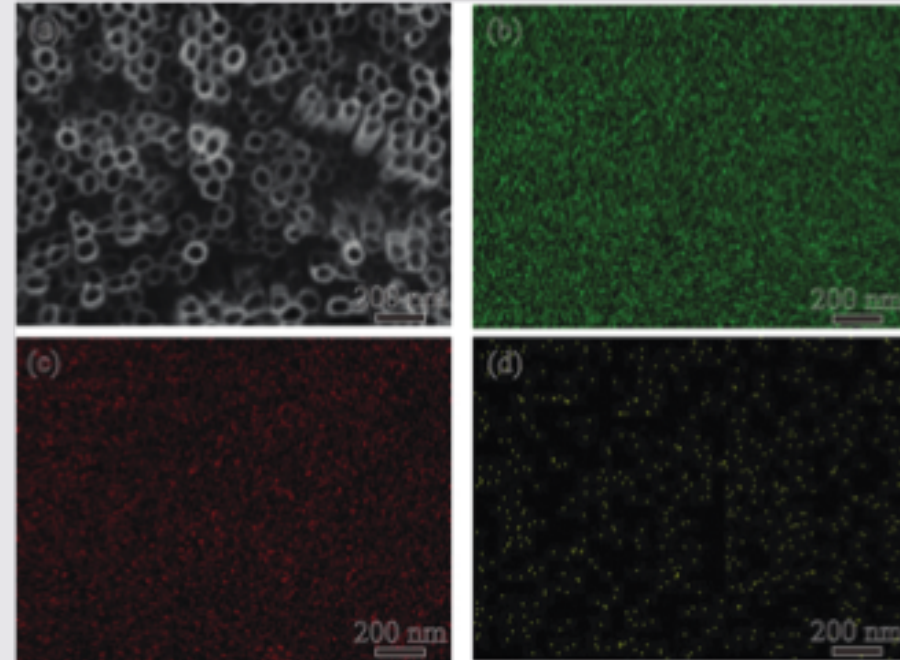


Figure 8. EDS analysis of ZnO-TNTs. (a) The selected area, (b) the distribution of Ti, (c) the distribution of O, (d) the distribution of Zn.

Chang F, et al. J Nanosci Nanotechnol. 2019 Apr 1;19(4):2070-2077.

Electrochemical Anodization

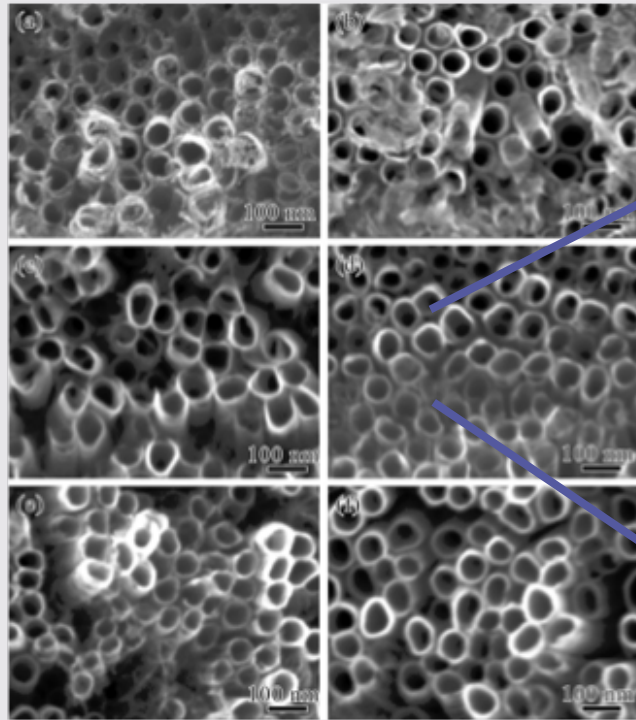


Figure 4. FE-SEM images representing the top view of ZnO-TNTs. (a) Undoped TNTs (spray-gold), (b) $1 \text{ mM} \cdot \text{L}^{-1}$ ZnO-TNTs, (c) $2 \text{ mM} \cdot \text{L}^{-1}$ ZnO-TNTs, (d) $3 \text{ mM} \cdot \text{L}^{-1}$ ZnO-TNTs, (e) $4 \text{ mM} \cdot \text{L}^{-1}$ ZnO-TNTs, (f) $5 \text{ mM} \cdot \text{L}^{-1}$ ZnO-TNTs.

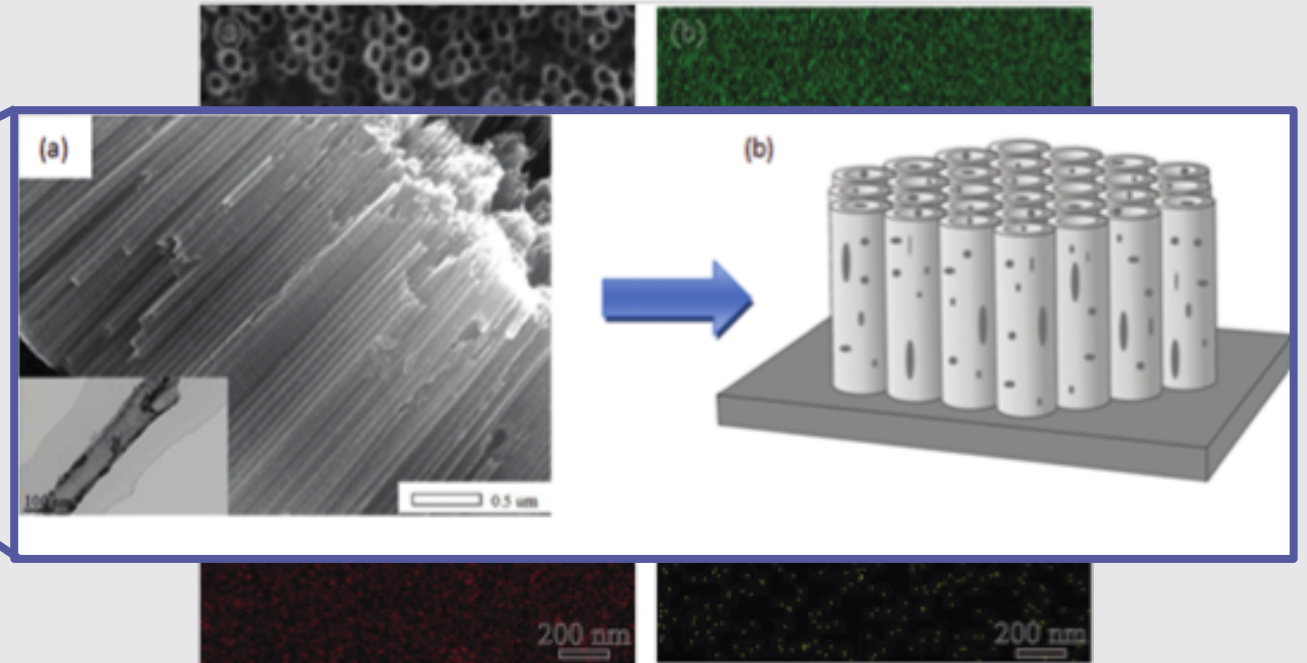


Figure 8. EDS analysis of ZnO-TNTs. (a) The selected area, (b) the distribution of Ti, (c) the distribution of O, (d) the distribution of Zn.

Chang F, et al. J Nanosci Nanotechnol. 2019 Apr 1;19(4):2070-2077.

Electrochemical Anodization

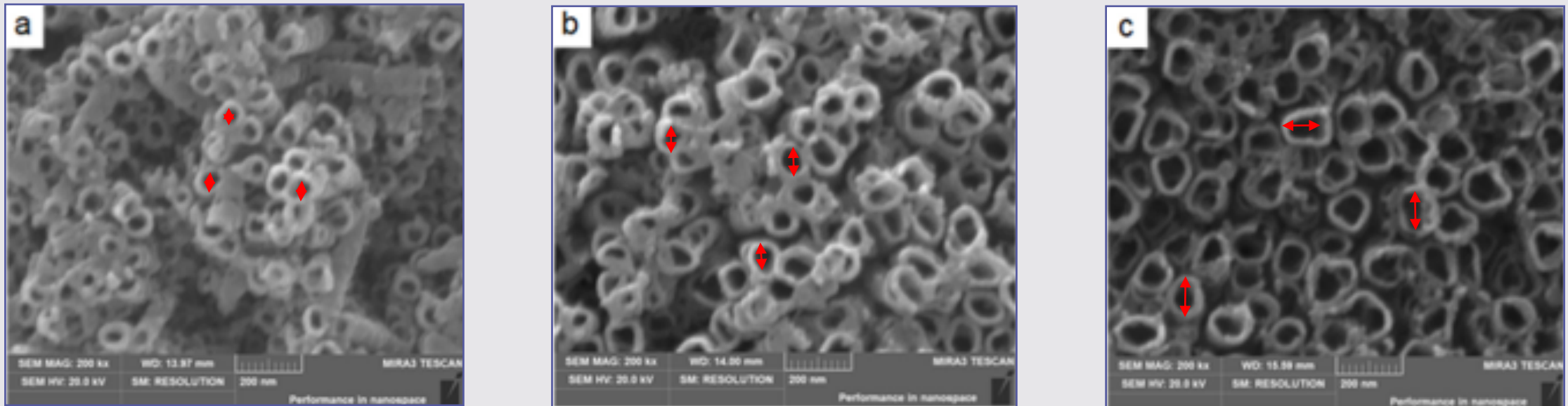
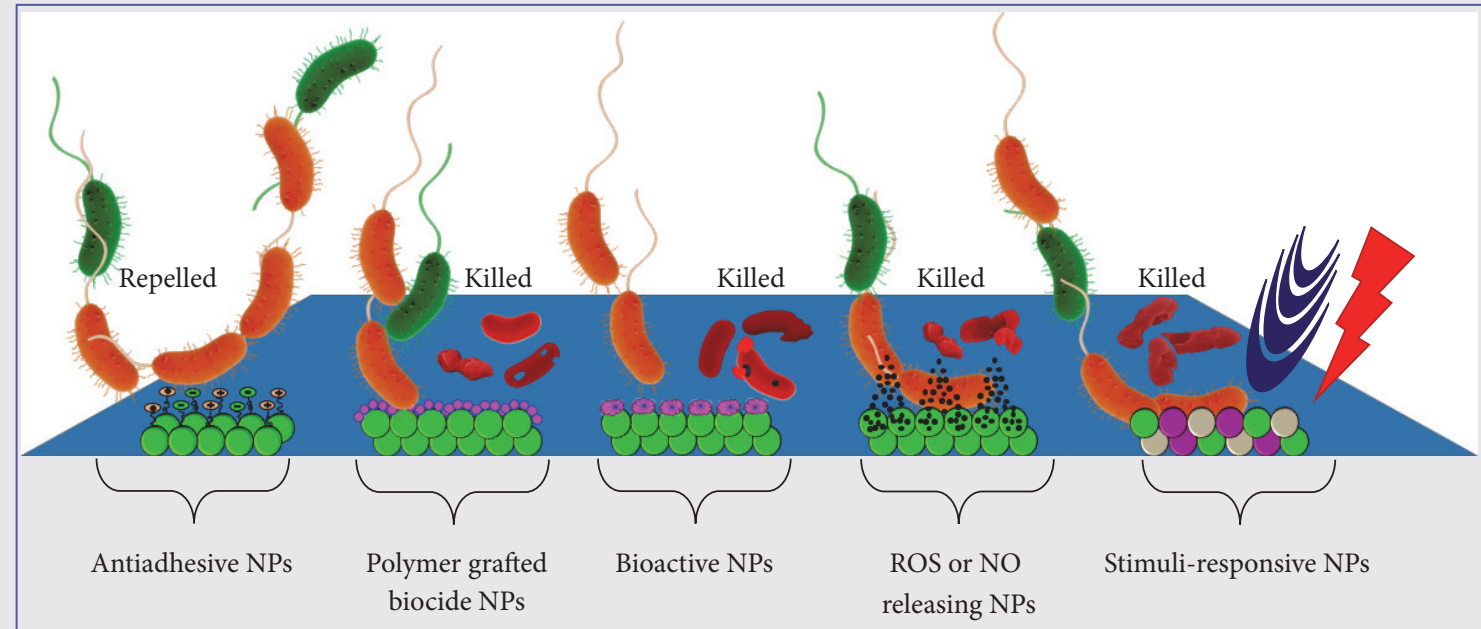


Figure 3. SEM images of nanotube arrays anodized at the following times: (a) 3 h, (b) 6 h and (c) 12 h, with inner diameters of approximately 44.5, 71.2 and 136.8 nm, respectively.

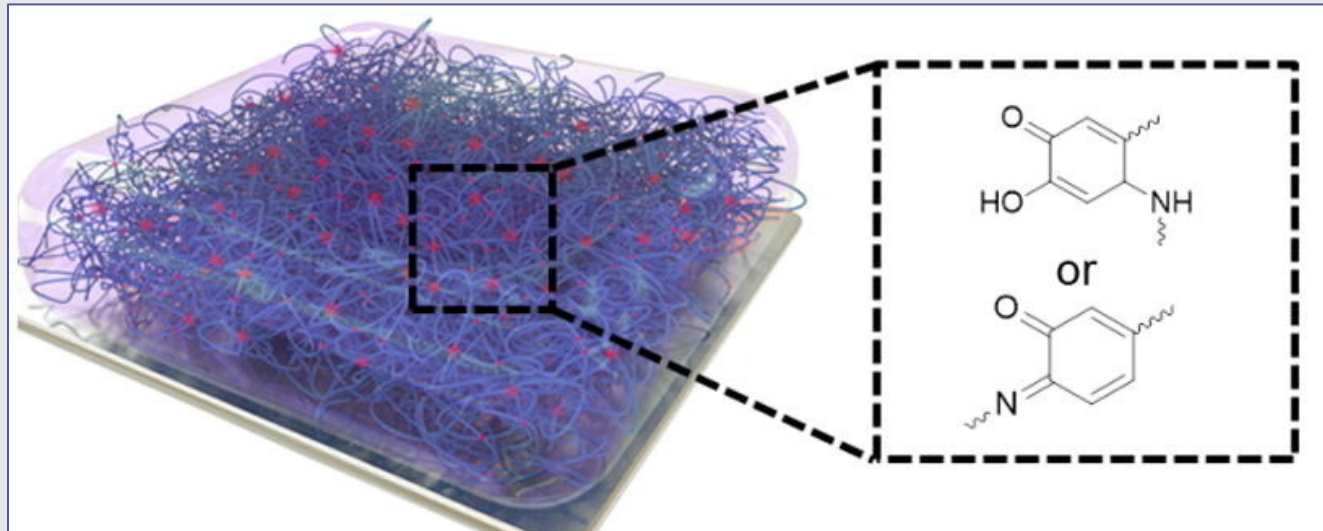
Modificación Superficies Catéteres

- Utilización polímeros con propiedades bactericidas.
- Bajo costo.
- Utilización de materiales “aprobados” por FDA.
- En conjunto con moléculas activas (Nps/ATB).



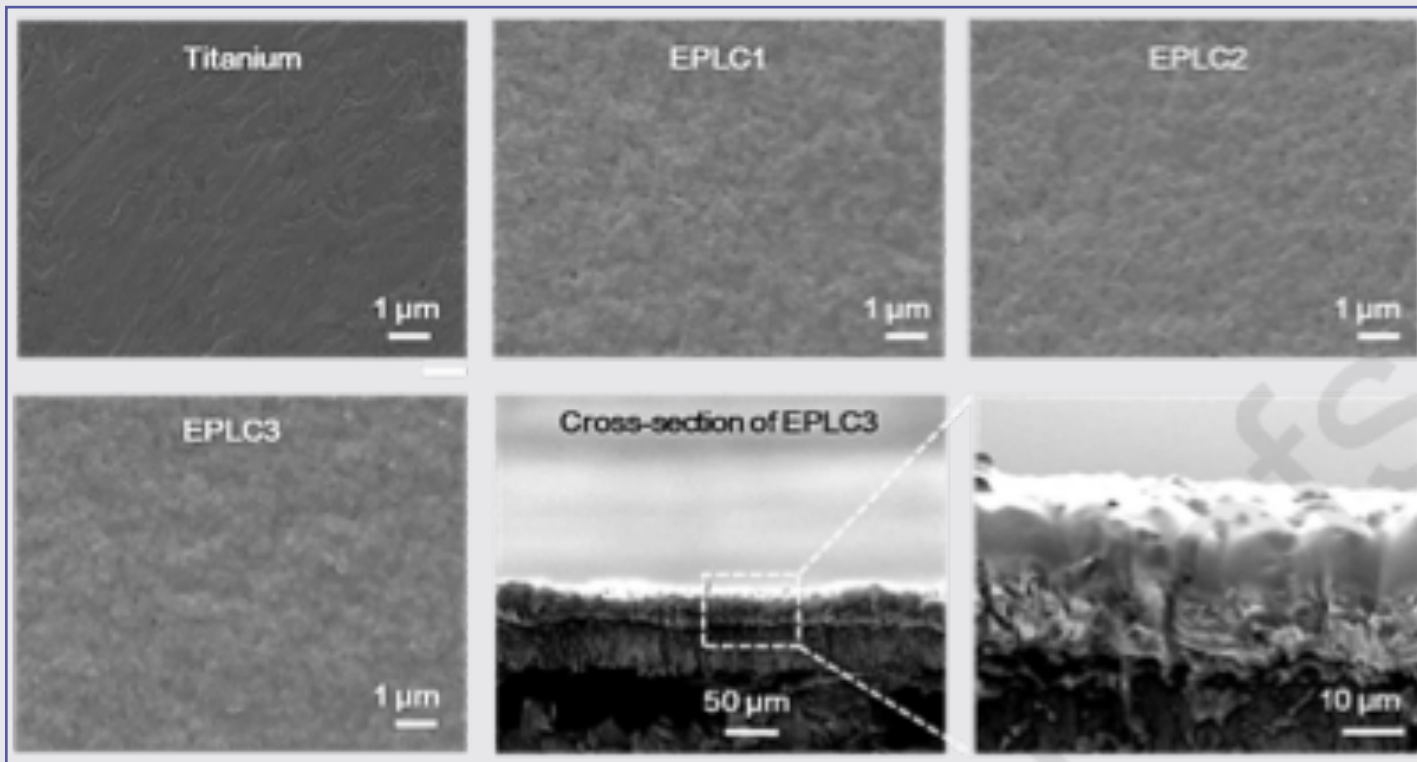
Ramasamy M, Lee J. Recent Nanotechnology Approaches for Prevention and Treatment of Biofilm-Associated Infections on Medical Devices. Biomed Res Int. 2016.

Modificación Superficies Catéteres



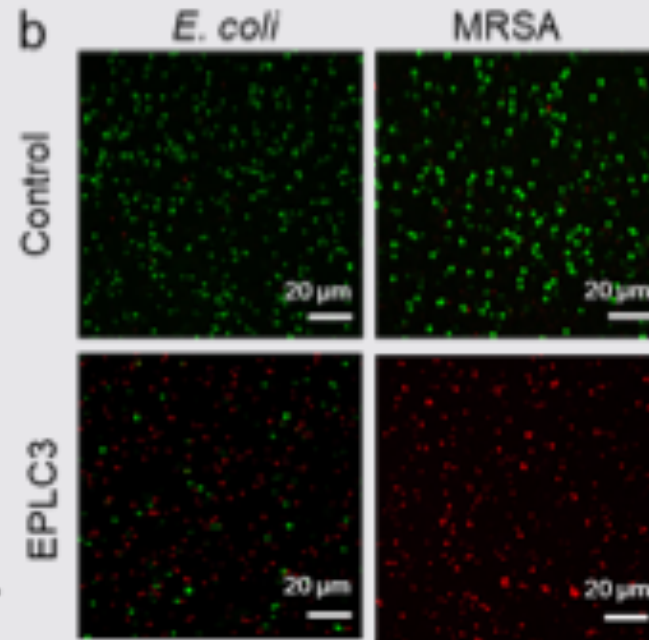
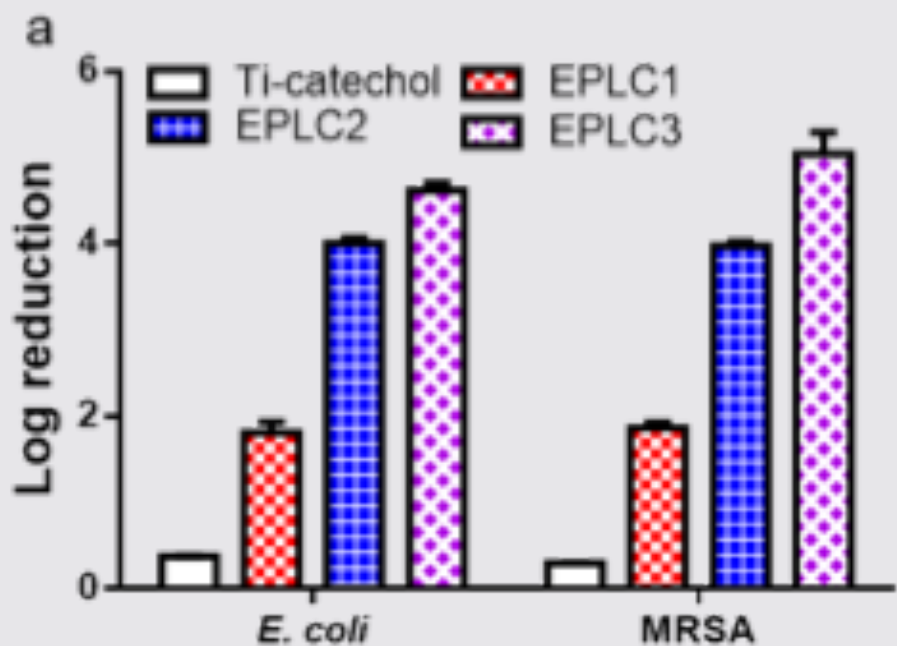
Characterization of mussel-inspired EPLC coatings. (a) SEM images of top surfaces of pristine Ti, and EPLC1/EPLC2/EPLC3 painted Ti substrate (Scale bar = 1 μm), and cross-section of EPLC3 coating on Ti substrate.

Modificación Superficies Catéteres



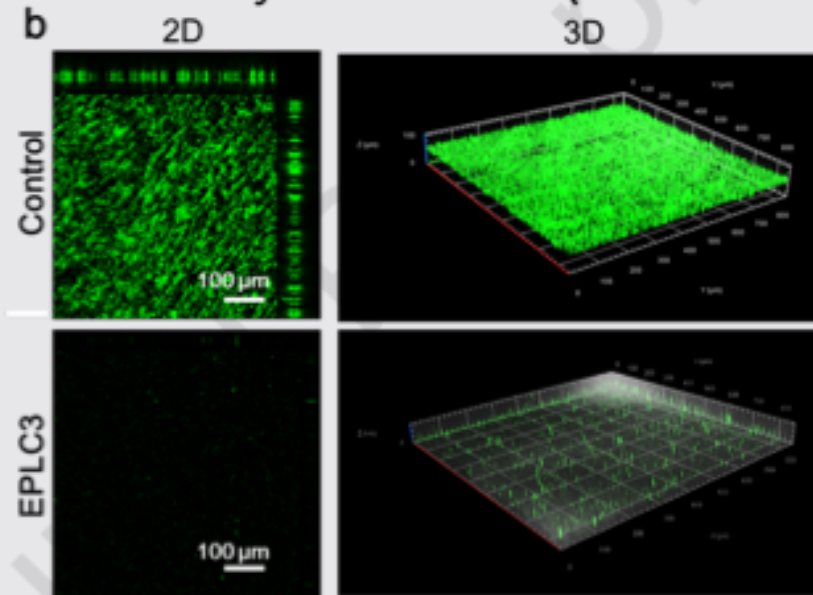
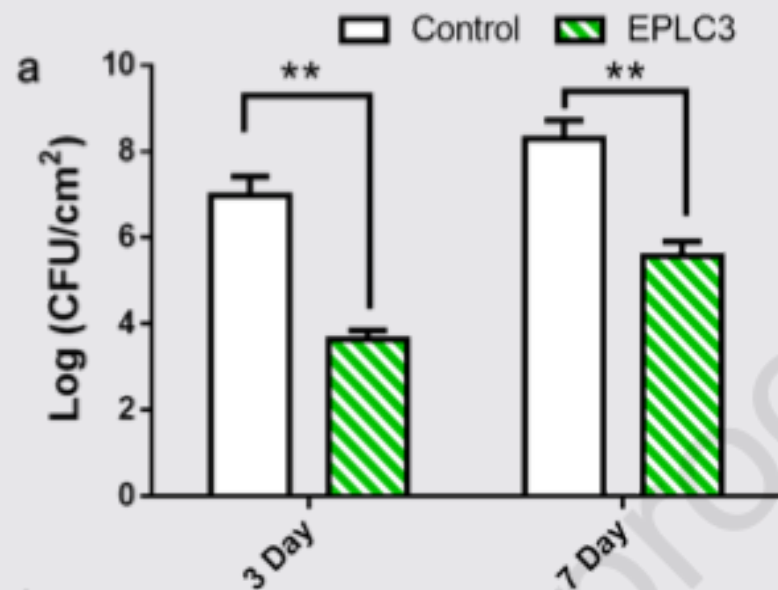
Characterization of mussel-inspired EPLC coatings. (a) SEM images of top surfaces of pristine Ti, and EPLC1/EPLC2/EPLC3 painted Ti substrate (Scale bar = 1 µm), and cross-section of EPLC3 coating on Ti substrate.

Modificación Superficies Catéteres



In vitro antimicrobial activities of EPLC coatings. (a) Bacterial reduction of EPLC coatings against *E. coli* and MRSA. Each data point represents the mean \pm standard deviation for three separate samples ($n = 3$). (b) Live/Dead bacterial viability assay of *E. coli* (Left) and MRSA (Right) on the control and EPLC3 coating.

Modificación Superficies Catéteres



In vitro anti-biofilm activity. (a) Bacterial (MRSA) count from biofilm at day 3 and day 7 ($n = 5$, $**p < 0.01$). Confocal microscopy images of MRSA growing on the surfaces of (b) control and EPLC3 painted quartz slides after 3 days. MRSA was stained using SYTOTM 9 green fluorescent nucleic acid stain. (Scale bar = 100 µm)

Miao Xu, et al. Chemical Engineering Journal, Volume 396, 2020.

FDA Guidelines

FDA **NO aprueba** el uso individual de materiales o recubrimientos, si no que el dispositivo médico terminado en su conjunto.

FDA evalúa:

- Análisis metalúrgico.
- Microestructura de la superficie modificada (grosor, forma, tamaño, diámetro o área, diámetro de poro, volumen).
- Propiedades físicas (dureza).
- Propiedades mecánicas (Resistencia/Fatiga).
- Biocompatibilidad.
- Información clínica.

[Consulta en línea: <https://www.fda.gov/regulatory-information/search-fda-guidance-documents/guidance-document-testing-orthopedic-implants-modified-metallic-surfaces-apposing-bone-or-bone>].

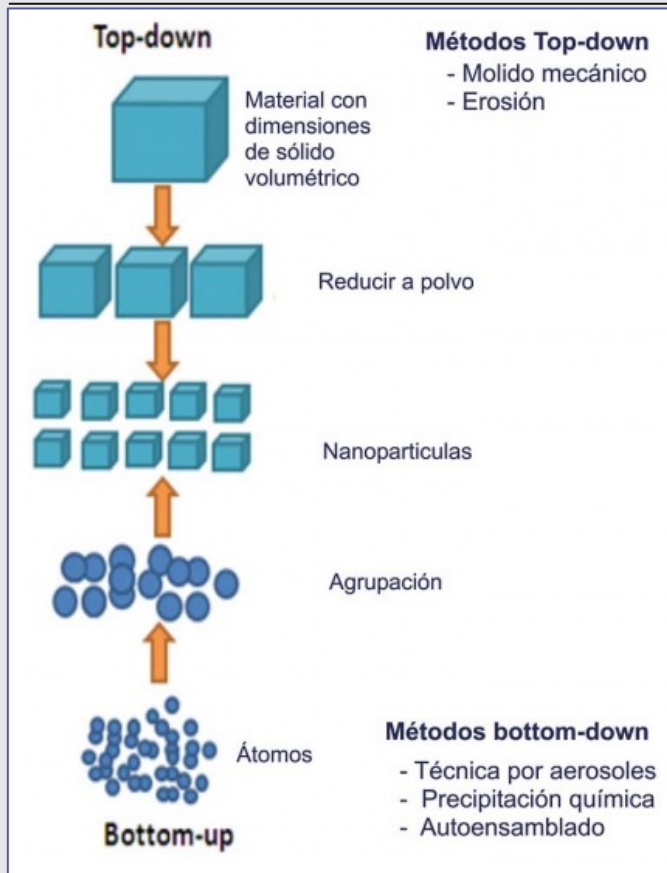
2

Nanotransportadores

3

Metodologías de Síntesis Generales

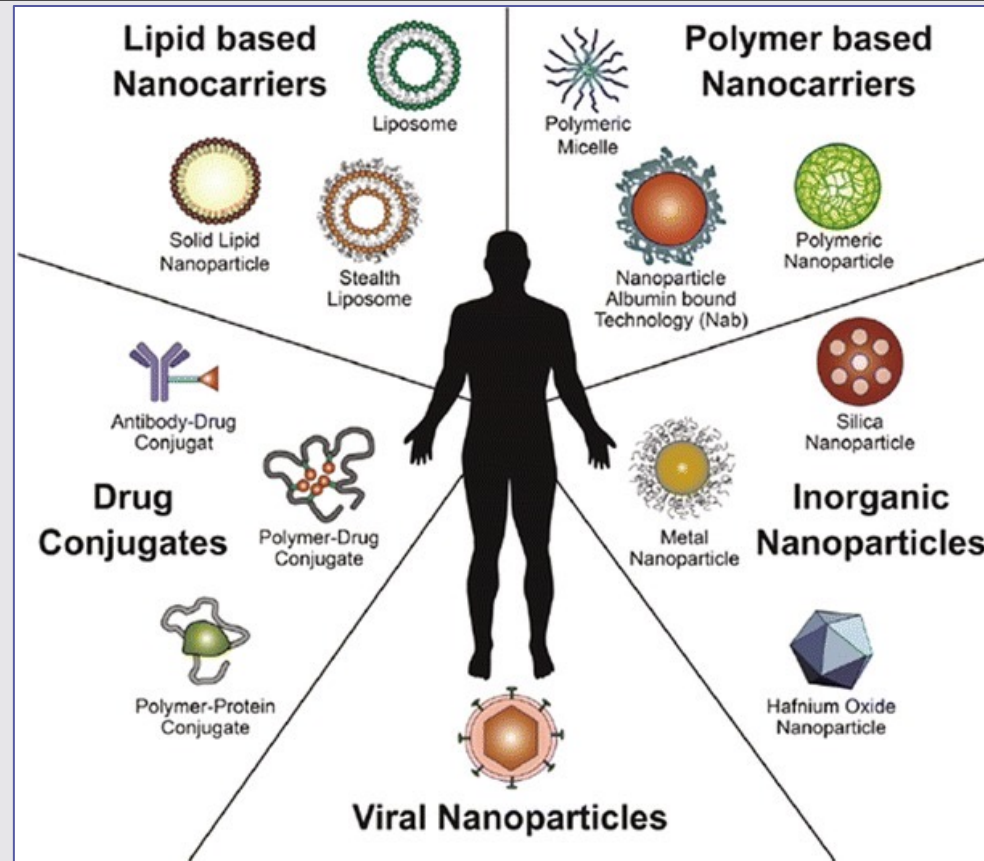
Nanotransportadores



Son sistemas coloidales en la escala nanométrica (1-100 nm), capaces de transportar drogas u otras sustancias de distinta naturaleza.

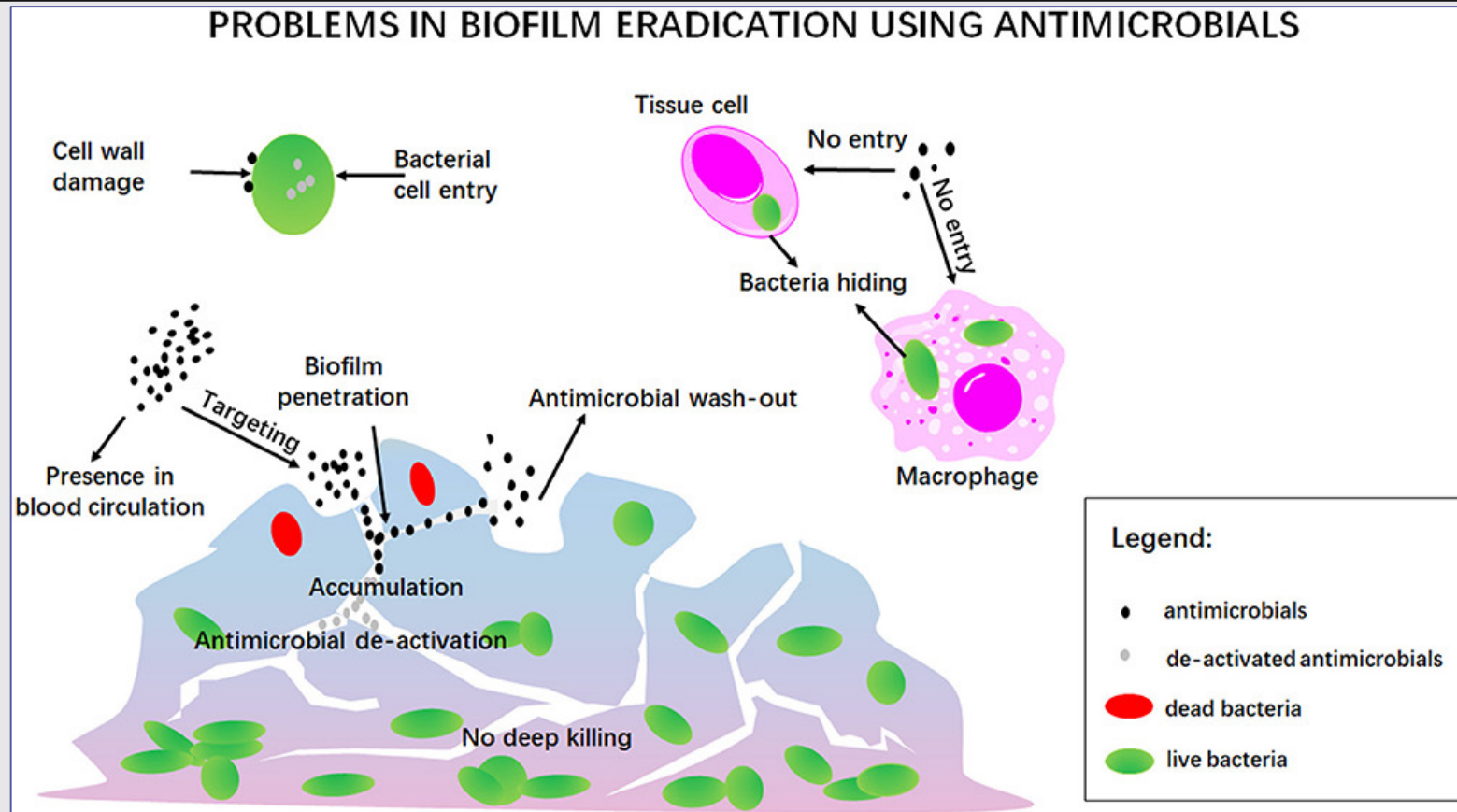
Din, F. et al. (2017). Effective use of nanocarriers as drug delivery systems for the treatment of selected tumors. *International journal of nanomedicine*, 12, 7291–7309.

Nanotransportadores



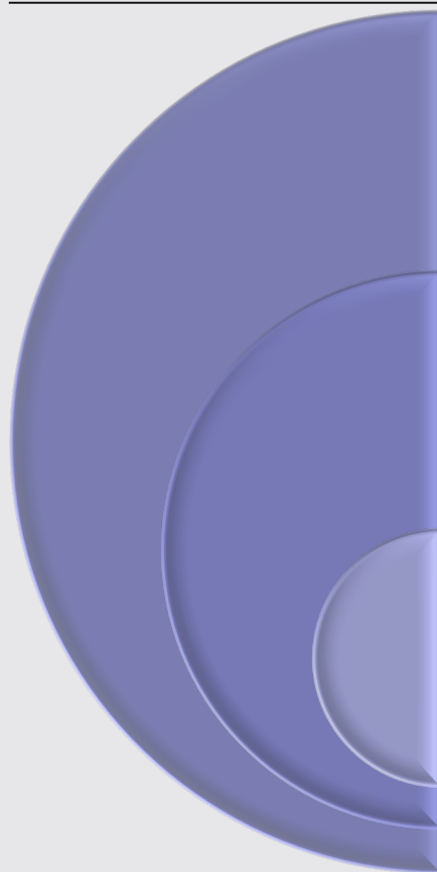
A. Wicki et al., Journal of Controlled Release **200**, 138 (2015).

Nanotransportadores de ATB



Wang DY, van der Mei HC, Ren Y, Busscher HJ, Shi L. Lipid-Based Antimicrobial Delivery-Systems for the Treatment of Bacterial Infections. Front Chem. 2020


Nanotransportadores de ATB



Utilizar menor concentración de ATB (uso racional)	<ul style="list-style-type: none">• Protección ATB
Modificación Superficial	<ul style="list-style-type: none">• Sitio acción específico.
Disrupción de BF	<ul style="list-style-type: none">• Células Plantónicas• Interacción/denaturación EPS

Din, F. et al. (2017). Effective use of nanocarriers as drug delivery systems for the treatment of selected tumors. *International journal of nanomedicine*, 12, 7291–7309.

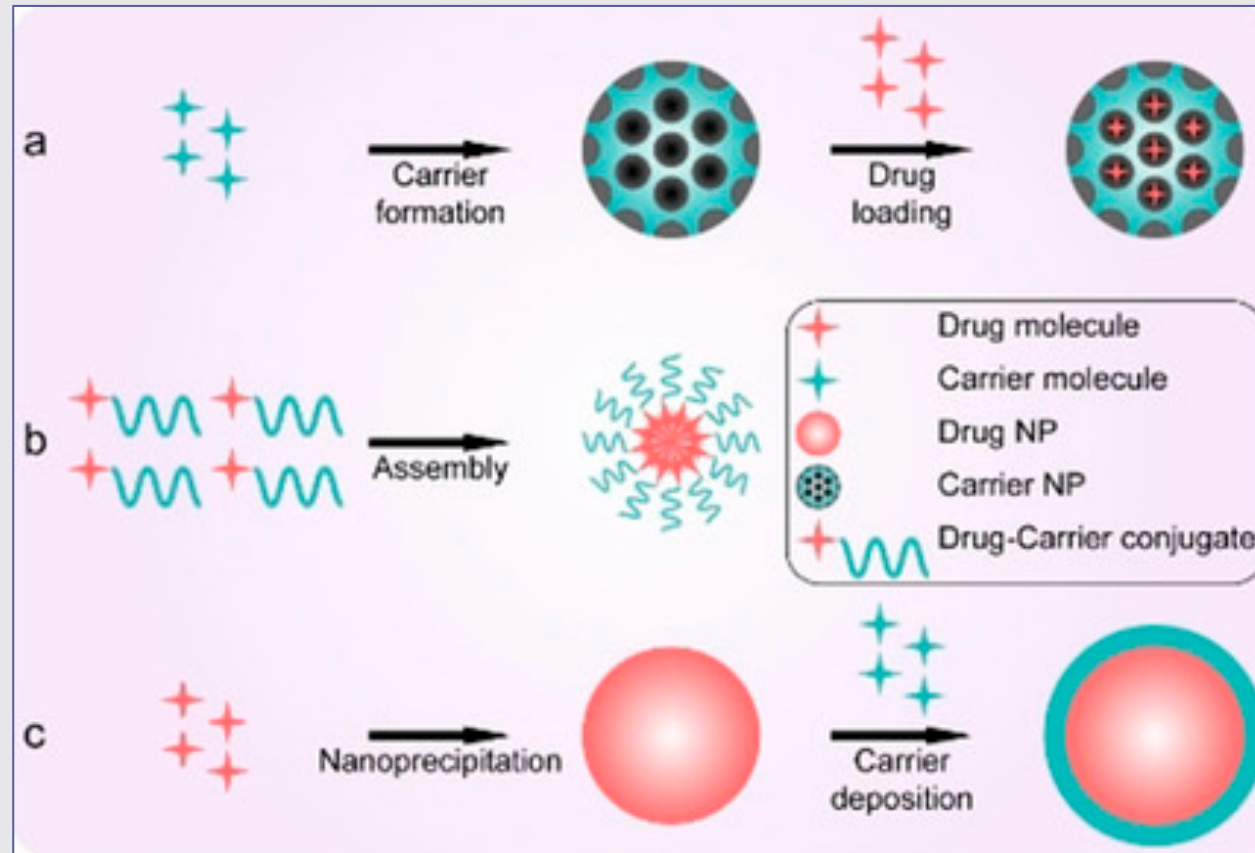
Nanotransportadores de ATB



	Strain	MIC against free antibiotics (mg/L)	MIC against liposomal encapsulated antibiotics (mg/L)	References		
M	Vancomycin				protección ATB	
	<i>E. coli</i>	512	6–25	Nicolosi et al., 2010	ón específico.	
		512	10.5			
	<i>Klebsiella</i>	512	25–50			
	<i>P. aeruginosa</i>	512	50			
			512	83.7		plantónicas on/denaturación EPS
	<i>Acinetobacter baumannii</i>	512	6–125			
	<i>S. aureus</i> (MRSA)	1	0.5	Bhise et al., 2018		
	Amikacin					
	<i>P. aeruginosa</i>	8	4	Mugabe et al., 2006		

Wang DY, van der Mei HC, Ren Y, Busscher HJ, Shi L. Lipid-Based Antimicrobial Delivery-Systems for the Treatment of Bacterial Infections. Front Chem. 2020

Nanotransportadores de ATB

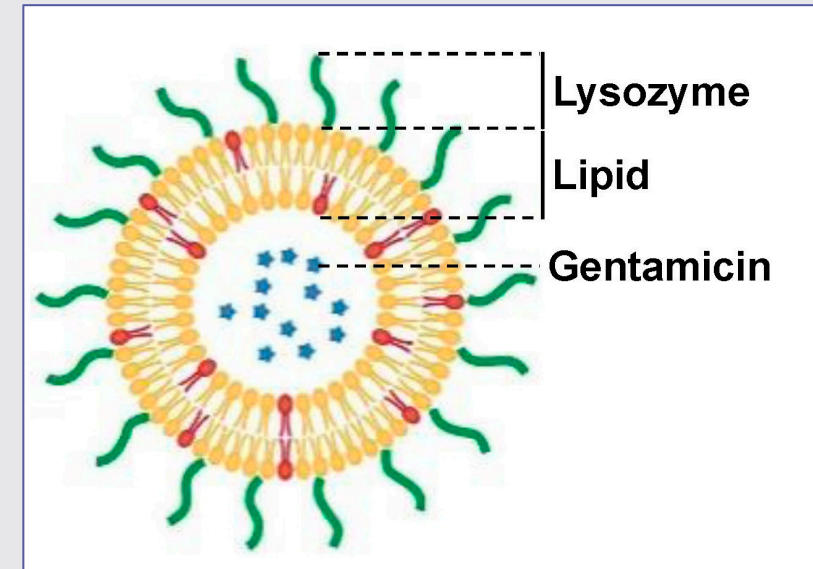
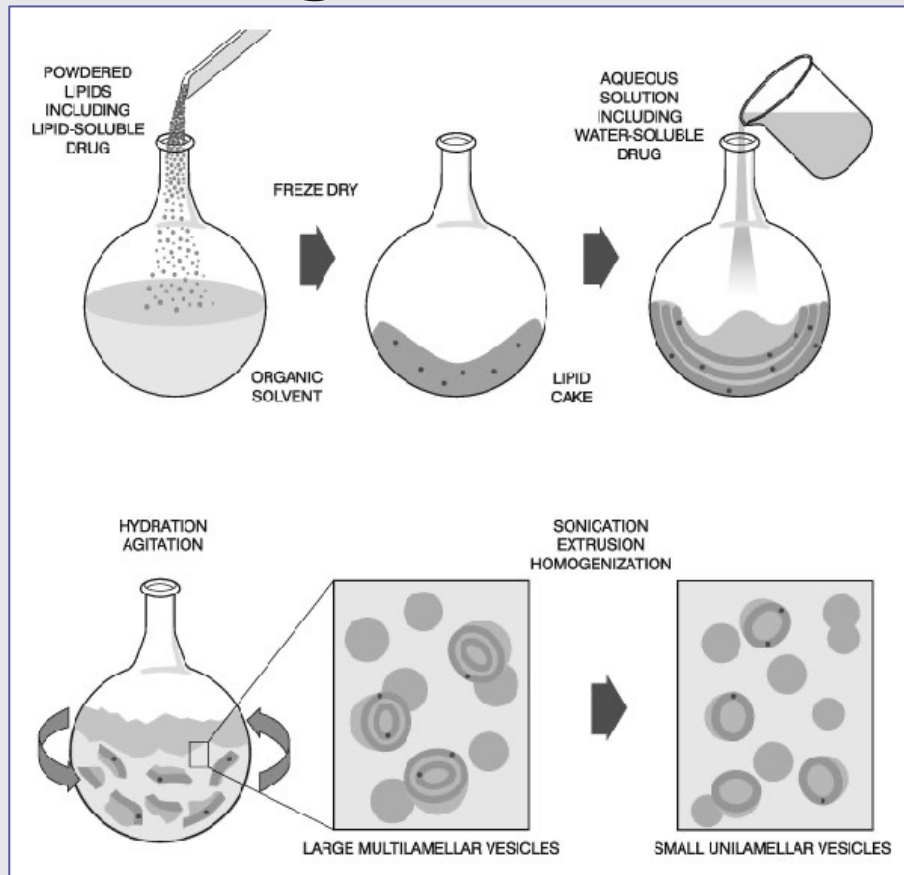


Y. Liu, G. Yang, S. Jin, L. Xu, C.-X. Zhao, *ChemPlusChem* **2020**, 85, 2143.

4

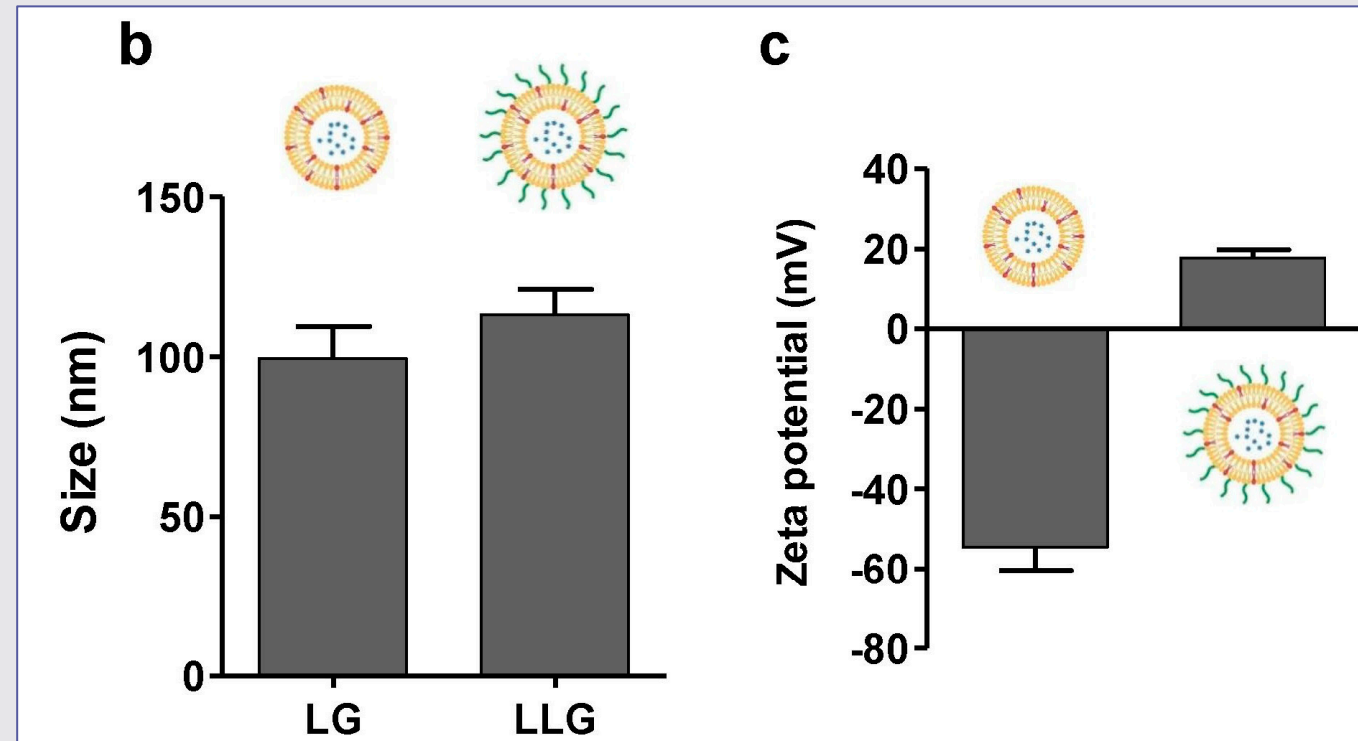
Algunos Ejemplos

Actividad antibiofilm de liposomas asociados a lisozima/gentamicina contra *P. aeruginosa* y *S. aureus*



Hou Y, Wang Z, Zhang P, Bai H, Sun Y, Duan J, Mu H. Lysozyme Associated Liposomal Gentamicin Inhibits Bacterial Biofilm. Int J Mol Sci. 2017 Apr 9;18(4):784.

Actividad antibiofilm de liposomas asociados a lisozima/gentamicina contra *P. aeruginosa* y *S. aureus*



Hou Y, Wang Z, Zhang P, Bai H, Sun Y, Duan J, Mu H. Lysozyme Associated Liposomal Gentamicin Inhibits Bacterial Biofilm. Int J Mol Sci. 2017 Apr 9;18(4):784.

Actividad antibiofilm de liposomas asociados a lisozima/gentamicina contra *P. aeruginosa* y *S. aureus*

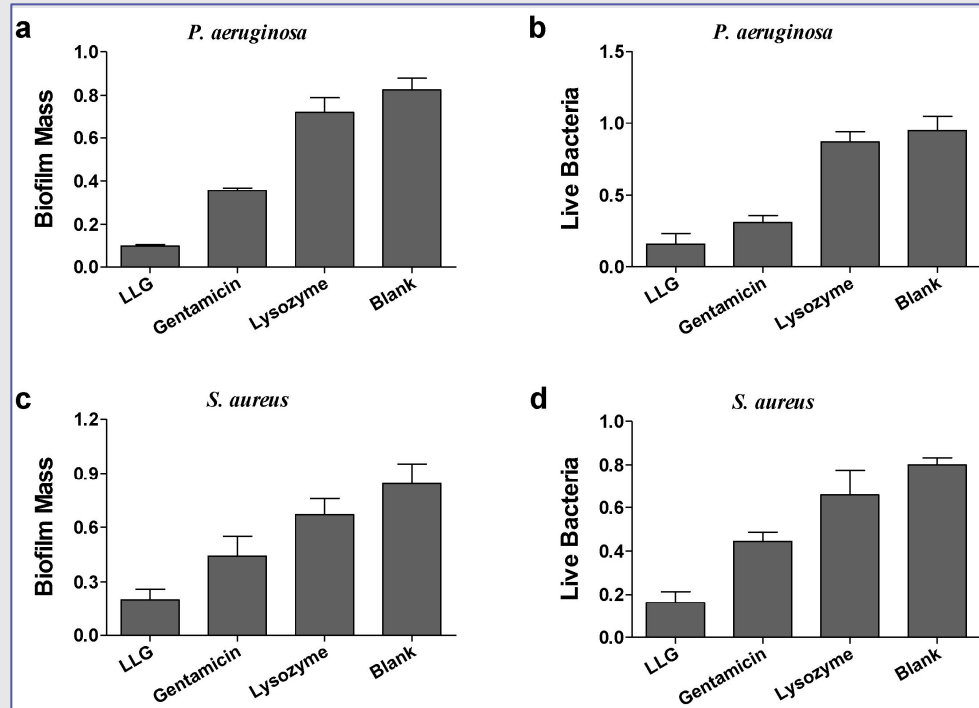


Figure 7. The inhibitory effects of LLG on *P. aeruginosa* (a,b) and *S. aureus* (c,d) biofilm formation.

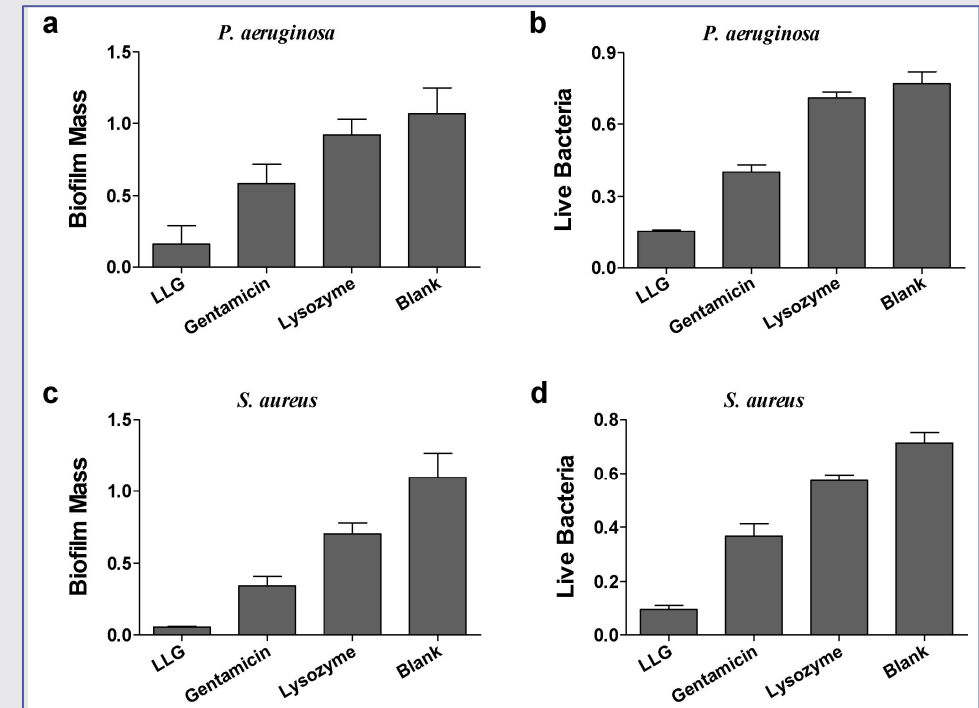


Figure 3. Crystal violet assay and 3-(4,5-dimethyl-thiazol-2-yl)-2,5-diphenyltetrazolium bromide (MTT) assay to assess the antibiofilm activity of LLG against *P. aeruginosa* biofilm (a,b) and *S. aureus* (c,d).

Actividad antibiofilm de liposomas asociados a lisozima/gentamicina contra *P. aeruginosa* y *S. aureus*

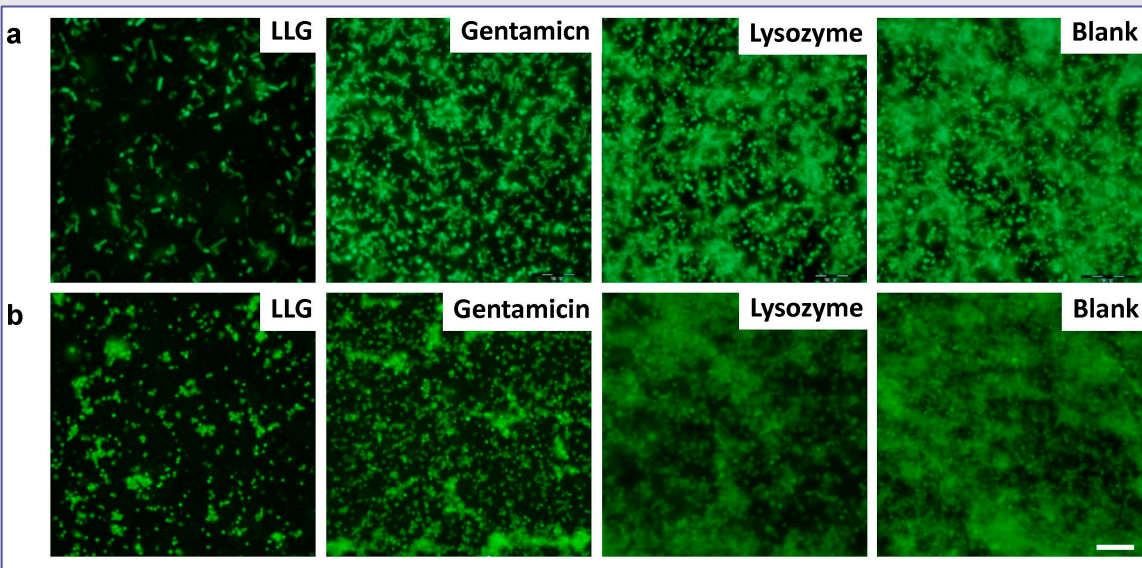


Figure 4. Fluorescence microscopy of *P. aeruginosa* (a) and *S. aureus* (b) biofilm. Biofilms incubated with tryptic soy broth (TSB) are used as control. Scale bars were 10 μ m.

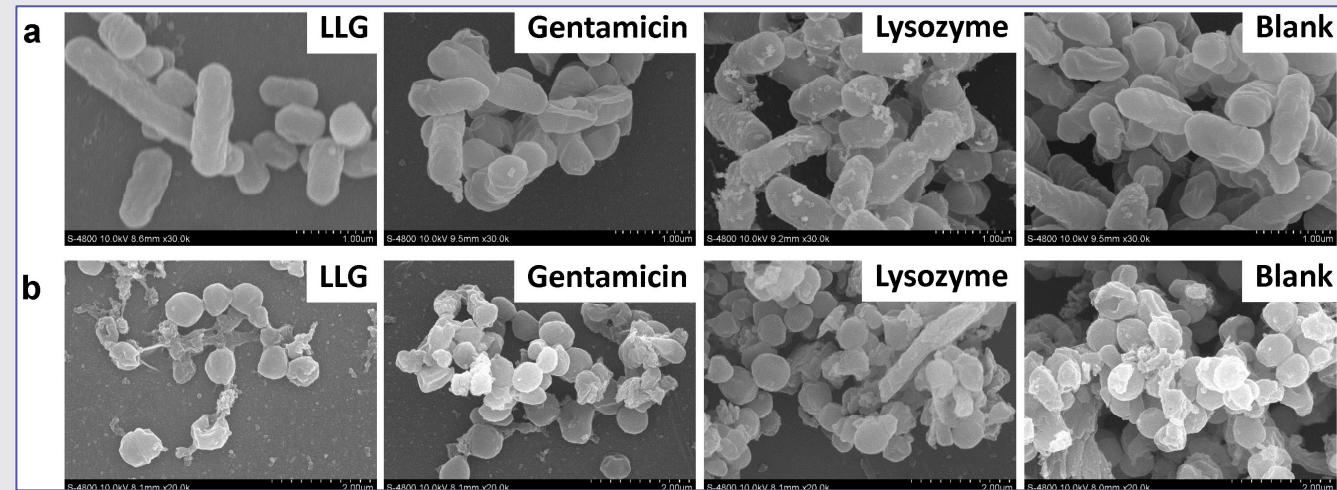
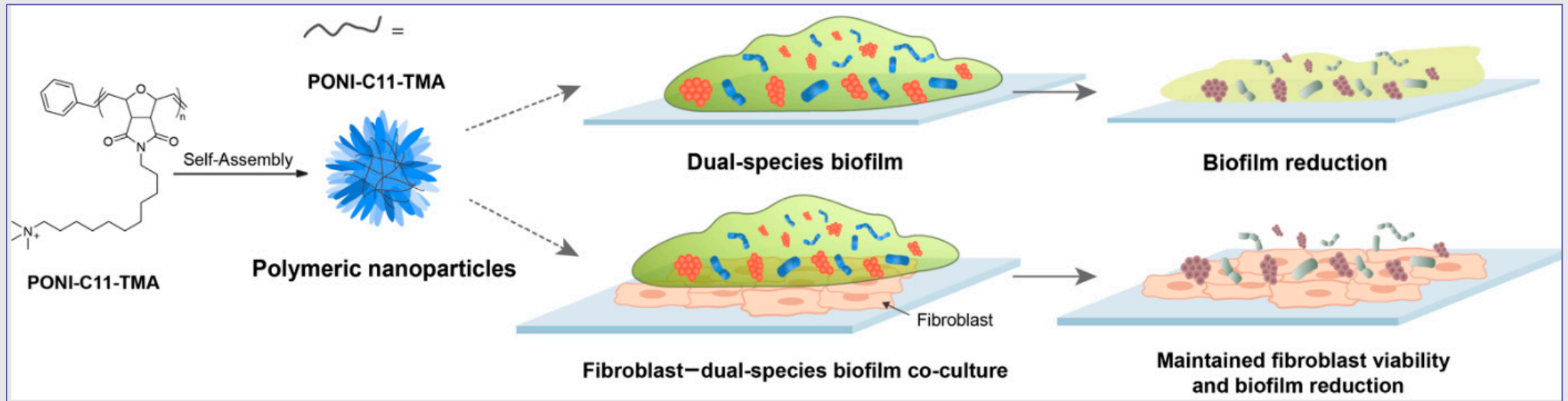


Figure 5. Scanning electron microscopy of *P. aeruginosa* (a) and *S. aureus* (b) biofilm. Biofilms incubated with TSB are used as control. Scale bars were 1 μ m.

Nanopartículas Poliméricas Activas contra biofilms *E. coli* y MRSA.



Scheme 1. Preparation and activity of PONI-C₁₁-TMA PNPs. The resulting PNPs significantly reduced established dual-species biofilms while maintaining fibroblast viability.

Nanopartículas Poliméricas Activas contra biofilms *E. coli* y MRSA.

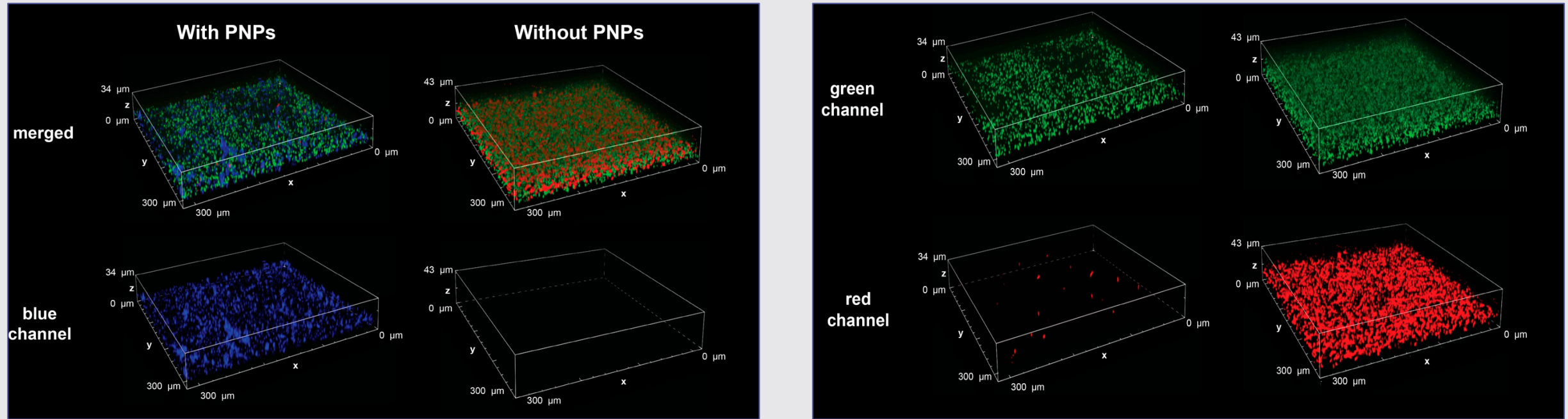


Figure 1. Representative 3D views of confocal image stacks of 4-day-old dual-species biofilm of DsRed-expressing *E. coli* (red channel) and GFP-expressing MRSA (green channel), coumarin blue-tagged PNPs (blue channel) and their overlay after treating the biofilms for 1 h with 1 μ M coumarin blue-tagged PNPs in M9 media.

Nanopartículas Poliméricas Activas contra biofilms *E. coli* y MRSA.

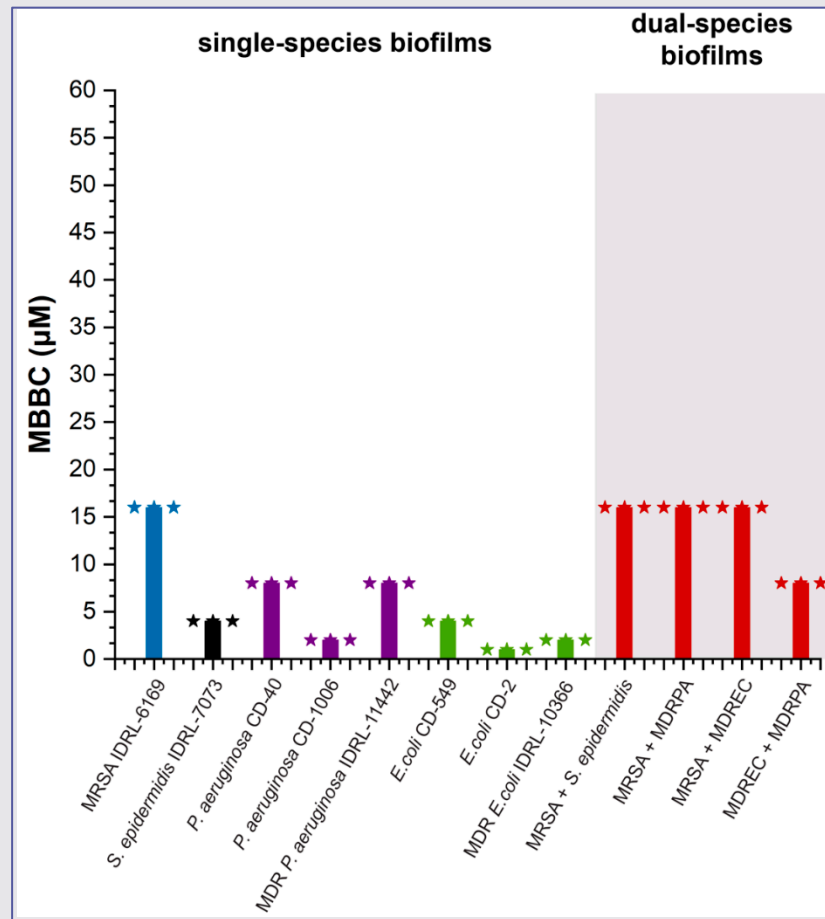


Figure 2. MBBC values of PNPs against mono-species (Gram-positive: MRSA, *S. epidermidis*; Gram-negative: *P. aeruginosa*, *E. coli*) and dual-species biofilms (MRSA IDRL-6169 + *S. epidermidis* IDRL-7073; MRSA IDRL-6169 + *P. aeruginosa* IDRL-11442; MRSA + *E. coli* IDRL-10366; *P. aeruginosa* IDRL-11442 + *E. coli* IDRL-10366). Bars represent average of three values, and stars represent individual measurements.

Nanopartículas Poliméricas Activas contra biofilms *E. coli* y MRSA.

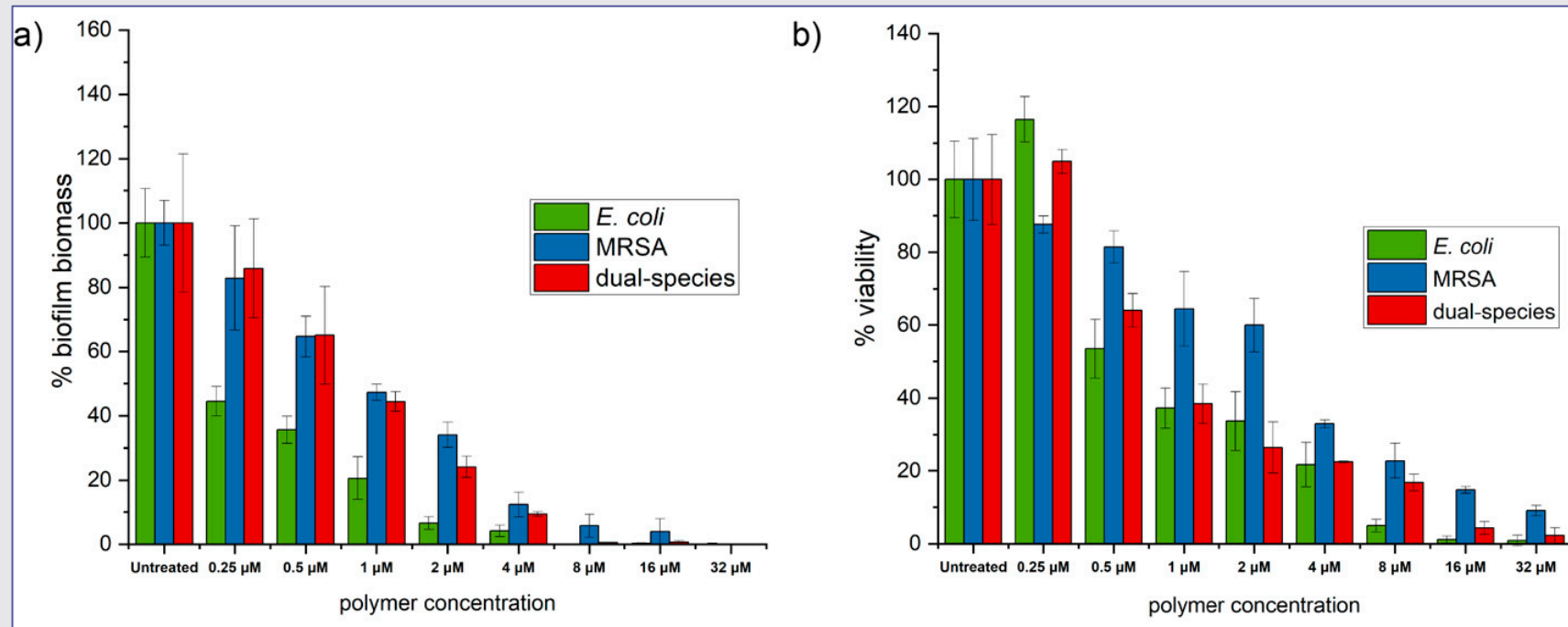


Figure 3. (a) Biomass and (b) bacteria viability of 2-day-old mono- and dual-species biofilms of MRSA IDRL-6169 + *E. coli* IDRL-10366 after 3 h treatment with PNPs. The data shown are averages of triplicates with the error bars indicating standard deviation.

Nanopartículas Poliméricas Activas contra biofilms *E. coli* y MRSA.

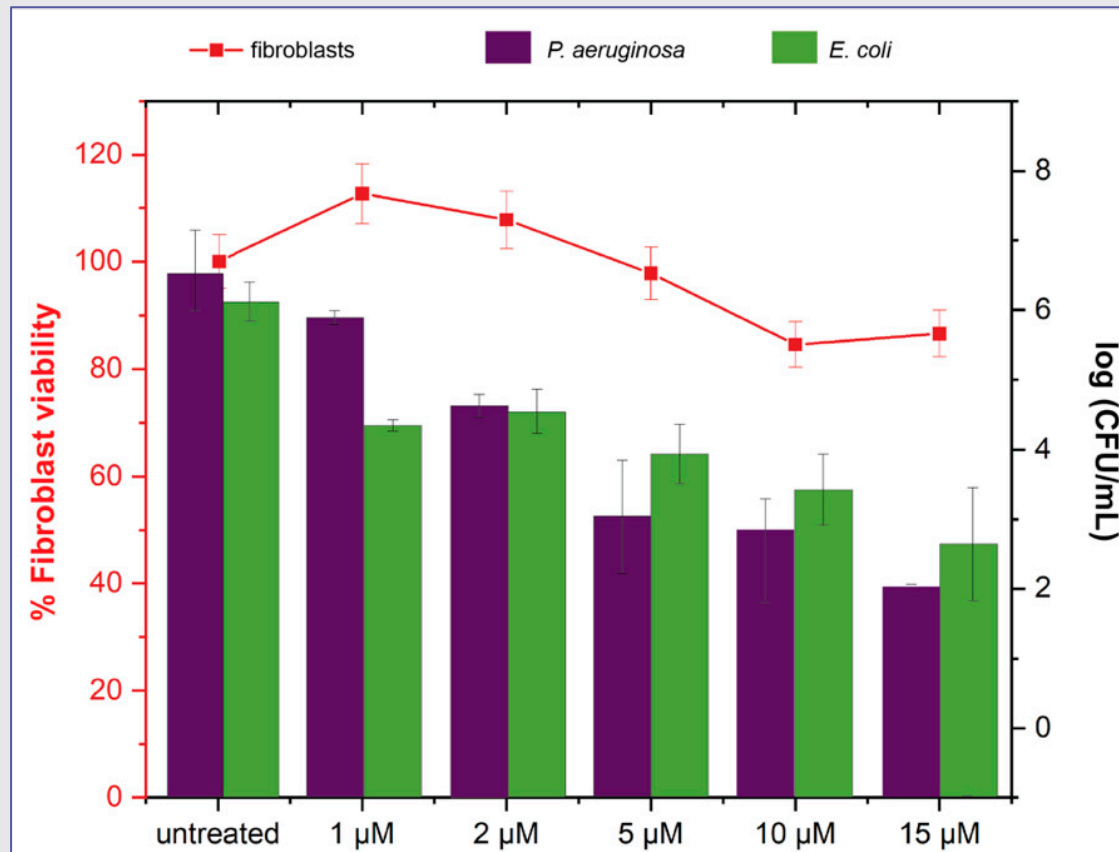


Figure 4. Viability of 3T3 fibroblast cells and *E. coli* DH5α + *P. aeruginosa* ATCC-19660 dual-species biofilms in the co-culture model after 3 h treatment with PNPs. Scatters and lines represent 3T3 fibroblast cell viability. Bars represent log₁₀ of colony-forming units in biofilms. Limit of quantification is 2 log₁₀. Data are averages of triplicates, with error bars indicating standard deviations.

Actividad antibiofilm de Silver Ultra-NanoClusters (SUNCs) contra *Helicobacter pylori*

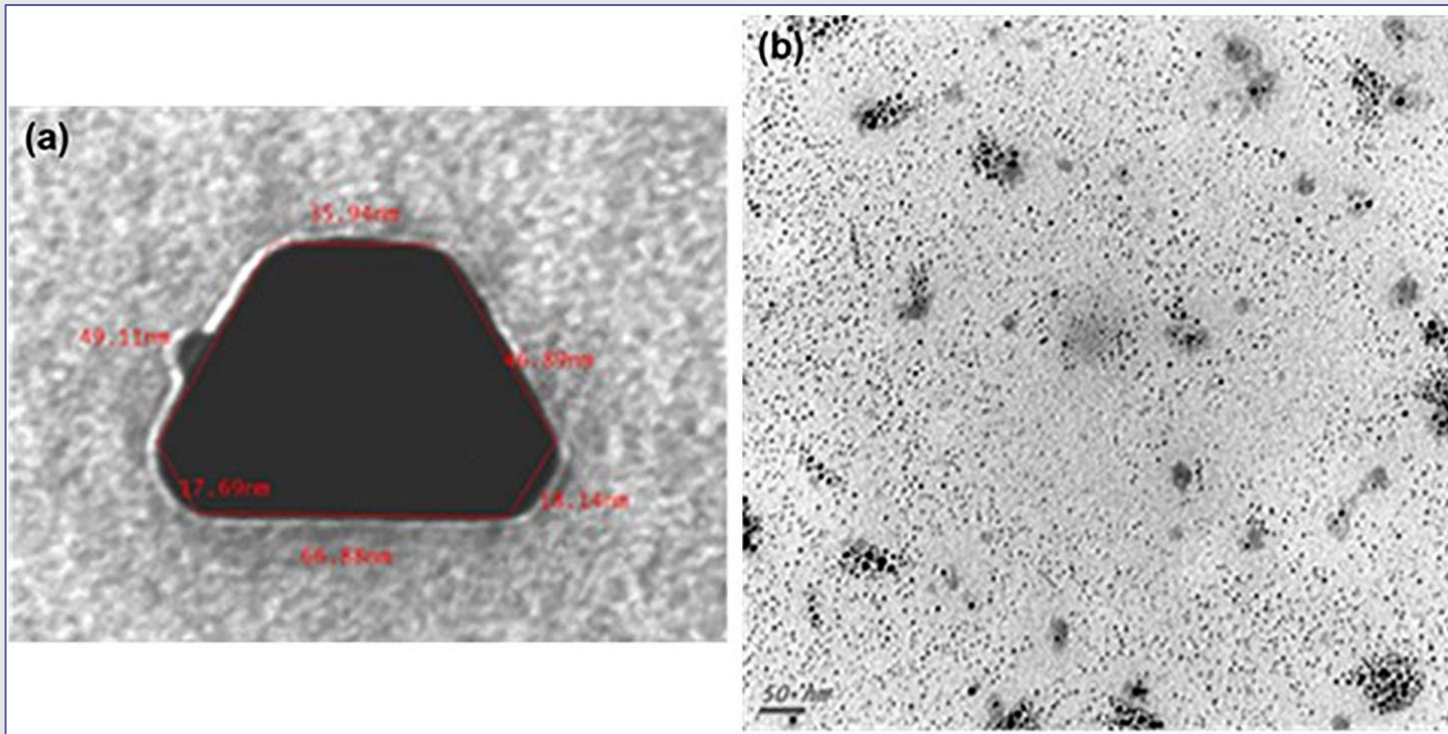


FIGURE 1: Transmission electron microscopy of SUNCs. SUNCs were electrochemically synthesized in ultrapure water. Large non-spherical nanocluster before filtration. Magnification: 250,000× (a); ultra-nanoclusters after filtration. A drop of 1:5 diluted stock solution of SUNCs was allowed to evaporate onto 300 mesh formvar-coated nickel grids, and then TEM image was taken at 75 kV by a ZEISS 109 microscope. Scale bar: 50 nm. Magnification: 85,000× (b).

Actividad antibiofilm de Silver Ultra-NanoClusters (SUNCs) contra *Helicobacter pylori*

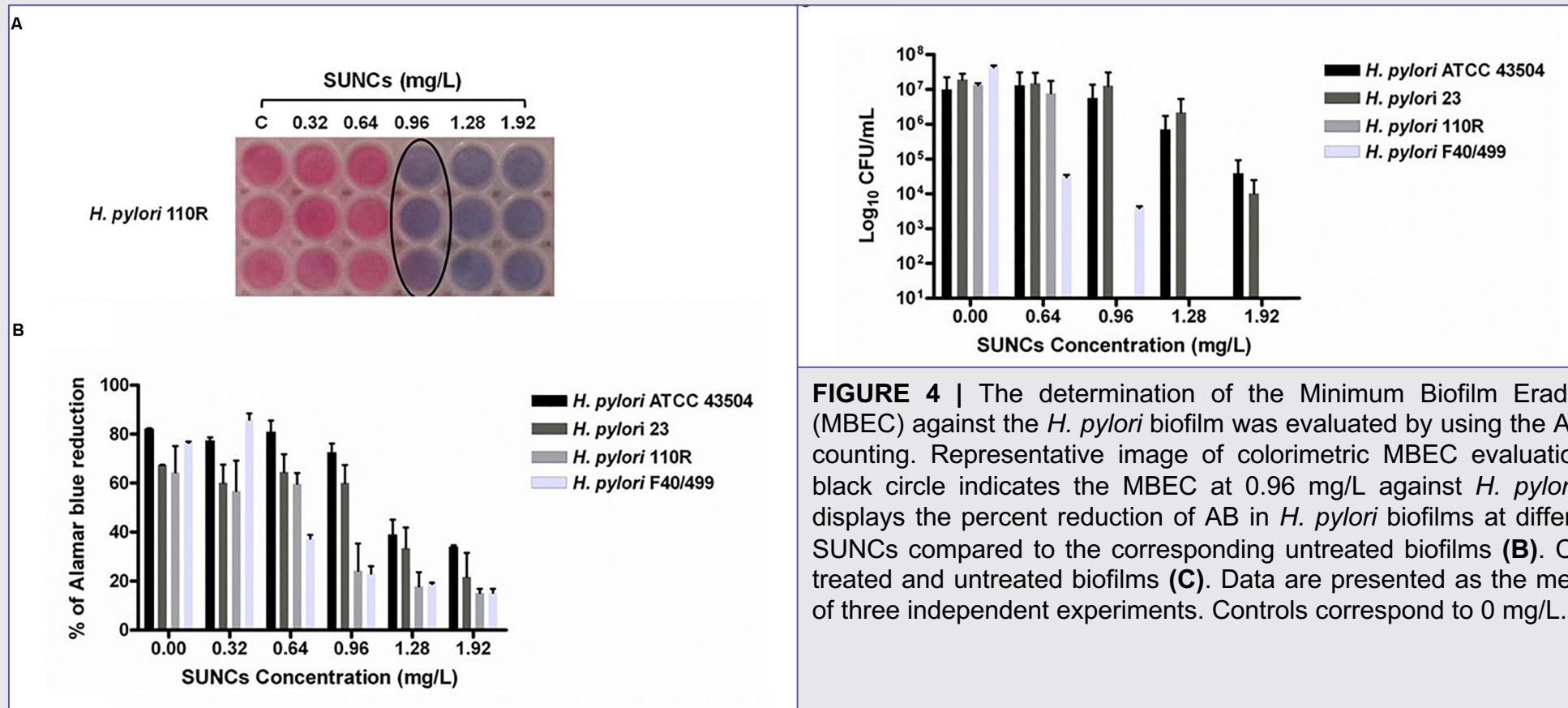


FIGURE 4 | The determination of the Minimum Biofilm Eradication Concentration (MBEC) against the *H. pylori* biofilm was evaluated by using the AB assay and the CFU counting. Representative image of colorimetric MBEC evaluation by using AB. The black circle indicates the MBEC at 0.96 mg/L against *H. pylori* 110R (**A**). The plot displays the percent reduction of AB in *H. pylori* biofilms at different concentrations of SUNCs compared to the corresponding untreated biofilms (**B**). CFU count of SUNCs-treated and untreated biofilms (**C**). Data are presented as the mean of three replicates of three independent experiments. Controls correspond to 0 mg/L.

Actividad antibiofilm de Silver Ultra-NanoClusters (SUNCs) contra *Helicobacter pylori*

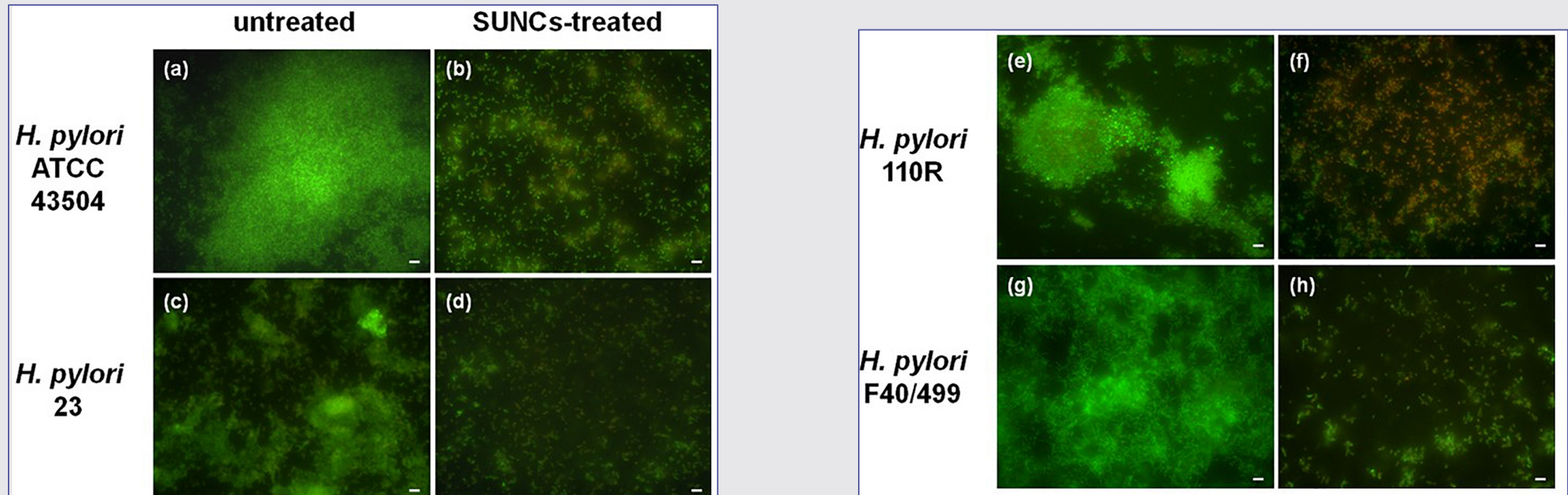


FIGURE 5 | Representative *H. pylori* biofilms stained with Live/Dead kit and analyzed using fluorescence microscopy. The green fluorescence indicates the live cells, whereas the red fluorescence indicates the dead cells or cells with a damaged cell wall. Panels (a,c,e,g) show the untreated *H. pylori* biofilms, while panels (b,d,f,h) show *H. pylori* biofilms treated with SUNCs at MBEC concentrations of 1.28 mg/L for *H. pylori* strains ATCC 43504 and 23, 0.96 mg/L for 110 R, and 0.64 mg/L for F40/499. Scale bar: 5 μ m.

Desafíos

Biocompatibilidad

Citotoxicidad a largo plazo

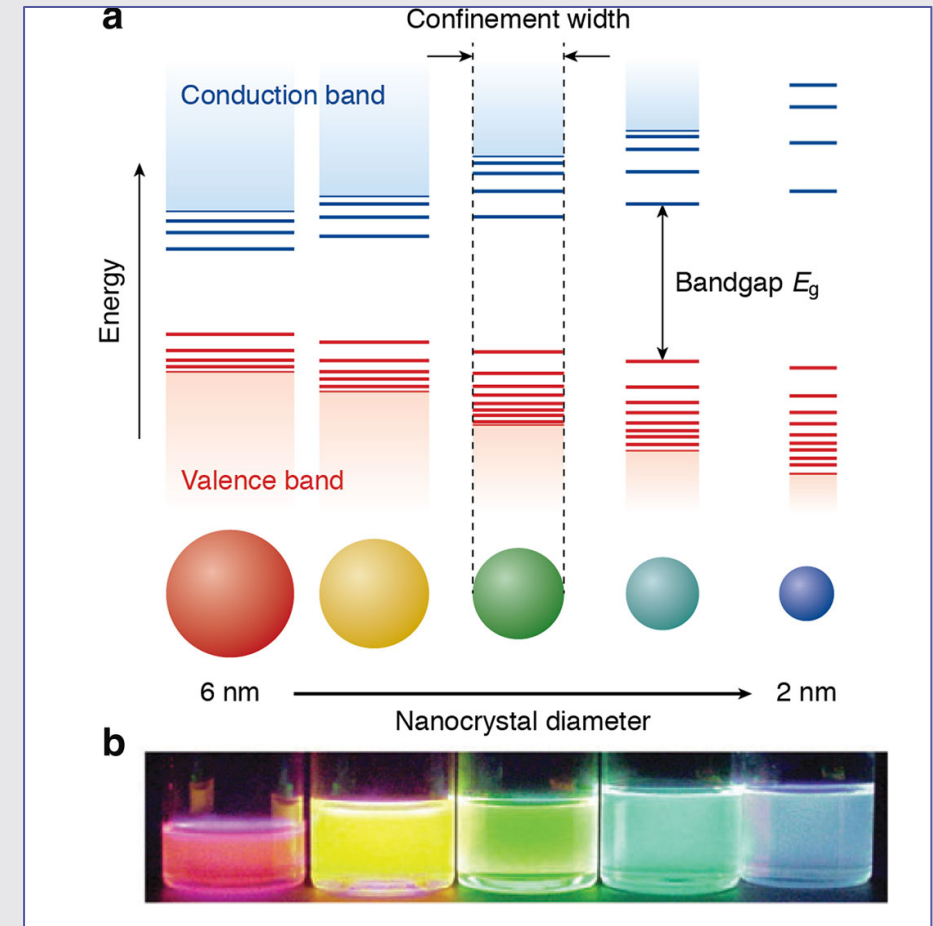
Acumulación Tejidos

Metabolización/Excreción

Quantum Dots

Son nanocristales de materiales semiconductores (grupos III–V y II–VI). Poseen propiedades ópticas particulares dadas por el confinamiento espacial de pares electrón-hueco (excitones) en una o más dimensiones (Efecto de confinamiento cuántico).

Este efecto es observado cuando el tamaño de estas partículas es cercano a la longitud de onda de Broglie para estos electrones, existiendo una transición de niveles de energía continuos a discretos.



Gracias!



CREDITS: This presentation template was created by **Slidesgo**, including icons by **Flaticon** and infographics & images by **Freepik**

